



OPEN ACCESS

EDITED BY

Asep K. Supriatna,
Universitas Padjadjaran, Indonesia

REVIEWED BY

Ebenezer Bonyah,
University of Education, Winneba,
Ghana
Pankaj Tiwari,
University of Kalyani, India

*CORRESPONDENCE

Fatmawati
✉ fatmawati@fst.unair.ac.id

SPECIALTY SECTION

This article was submitted to
Mathematical Biology,
a section of the journal
Frontiers in Applied Mathematics and
Statistics

RECEIVED 11 November 2022

ACCEPTED 07 December 2022

PUBLISHED 06 January 2023

CITATION

Rois MA, Fatmawati, Alfiniyah C and
Chukwu CW (2023) Dynamic analysis
and optimal control of COVID-19 with
comorbidity: A modeling study of
Indonesia.
Front. Appl. Math. Stat. 8:1096141.
doi: 10.3389/fams.2022.1096141

COPYRIGHT

© 2023 Rois, Fatmawati, Alfiniyah and
Chukwu. This is an open-access article
distributed under the terms of the
[Creative Commons Attribution License
\(CC BY\)](https://creativecommons.org/licenses/by/4.0/). The use, distribution or
reproduction in other forums is
permitted, provided the original
author(s) and the copyright owner(s)
are credited and that the original
publication in this journal is cited, in
accordance with accepted academic
practice. No use, distribution or
reproduction is permitted which does
not comply with these terms.

Dynamic analysis and optimal control of COVID-19 with comorbidity: A modeling study of Indonesia

Muhammad Abdurrahman Rois¹, Fatmawati^{1*}, Cicik Alfiniyah¹ and Chidozie W. Chukwu²

¹Department of Mathematics, Faculty of Science and Technology, Universitas Airlangga, Surabaya, Indonesia, ²Department of Mathematics, Wake Forest University, Winston-Salem, NC, United States

Comorbidity is defined as the coexistence of two or more diseases in a person at the same time. The mathematical analysis of the COVID-19 model with comorbidities presented includes model validation of cumulative cases infected with COVID-19 from 1 November 2020 to 19 May 2021 in Indonesia, followed by positivity and boundedness solutions, equilibrium point, basic reproduction number (R_0), and stability of the equilibrium point. A sensitivity analysis was carried out to determine how the parameters affect the spread. Disease-free equilibrium points are asymptotically stable locally and globally if $R_0 < 1$ and endemic equilibrium points exist, locally and globally asymptotically stable if $R_0 > 1$. In addition, this disease is endemic in Indonesia, with $R_0 = 1.47$. Furthermore, two optimal controls, namely public education and increased medical care, are included in the model to determine the best strategy to reduce the spread of the disease. Overall, the two control measures were equally effective in suppressing the spread of the disease as the number of COVID-19 infections was significantly reduced. Thus, it was concluded that more attention should be paid to patients with COVID-19 with underlying comorbid conditions because the probability of being infected with COVID-19 is higher and mortality in this population is much higher. Finally, the combined control strategy is an optimal strategy that provides an effective guarantee to protect the public from the COVID-19 infection based on numerical simulations and cost evaluations.

KEYWORDS

COVID-19, comorbidity, stability, sensitivity analysis, optimal control, cost evaluation

1. Introduction

The COVID-19 virus was reported in the Wuhan-Hubei Province of China in December 2019 and was spread rapidly to various parts of the world [1–6]. Symptoms are usually mild and appear gradually. In general, the symptoms of COVID-19 are fever, dry cough, and tiredness. In addition, there are other symptoms such as chest pain and tenderness, nasal congestion, headache, conjunctivitis, diarrhea, loss of sense of taste or smell, skin rash, or discoloration of the fingers or toes [6]. The symptoms experienced are usually mild and appear gradually. Furthermore, moderate and severe infection symptoms can occur in

humans and appear gradually, such as having fever and cough accompanied by difficulty in breathing or shortness of breath, chest pain, and others [1, 6]. Individuals with previous comorbidity (such as diabetes, lung, and heart disease) are more likely to develop severe disease with stronger COVID-19 symptoms than individuals who do not have a comorbidity [7, 8]. In the case of COVID-19 comorbidity in Indonesia, 12 different diseases have been recorded, which range from the most at risk to the least at risk, namely hypertension, diabetes mellitus, heart, pregnancy, lung, kidney, immune disorders, cancer, other respiratory disorders, asthma, tuberculosis, and liver [9].

The first case in Indonesia was reported directly by President Jokowi Widodo on 2 March 2020 and there were as many as two people infected, namely a mother and child suspected of contracting it from a Japanese citizen [10]. Data from web [11], on 2 October 2020, to be precise, indicate that Indonesia was ranked 23 out of 215 countries reported being infected with 295,499 confirmed cases, 10,972 reported deaths, and 221,340 reported recoveries. Meanwhile, according to data on 14 June 2021, Indonesia was ranked 18 out of 222 countries reported being infected, with 1,919,547 confirmed cases, 53,116 reported deaths, and 1,751,234 reported recoveries.

The increasing number of COVID-19 cases requires a control strategy to control the COVID-19 outbreak. Control technique isolation and individual quarantine are the most efficient measures whenever a new outbreak occurs in a region without a vaccine or therapy [12, 13]. Several appeals or mitigations from WHO to control COVID-19 are social distancing, use of masks in public places, and intensive contact tracing (tracing) followed by quarantine of individuals who have the potential to contract the disease, and isolation of infected individuals in hospitals or independently [14]. Therefore, public education plays an important role in controlling the outbreak because it can convey information regarding how to prevent and reduce the transmission of COVID-19.

Furthermore, it is necessary to use mathematical modeling to determine the spread of COVID-19 infection and whether the control measures are effective. WHO also acknowledges that mathematical modeling can help health decision-makers (doctors or health professionals) and policymakers make decisions or find solutions (governments) [15]. The Susceptible-Infected-Removed (SIR) model is a mathematical representation of how diseases spread. The SIR model was first developed in 1927 by Kermack and McKendrick, who established it as a reference work and contributed significantly to the development of the mathematical theory of disease transmission [16, 17]. Several studies are related to the spread of disease, for example, research on the Coronavirus that caused SARS [18] and MERS [19, 20].

Soewono [21] applied the SEIR model, which has four subpopulations: susceptible (S), exposed (E), infected (I),

and recovered (R), to simulate the spread of COVID-19. This model is an improvement on the SIR COVID-19 model. Furthermore, Das et al. [22] add a subpopulation of C (infected with comorbidity), so that the population is divided into five subpopulations, namely S , E , I , C , and R . The comorbidity referred to in this study is a general congenital disease, while research from Omame et al. [23] also proposed a comorbidity COVID-19 model, Omame et al. model coinfection with comorbidities (especially diabetes mellitus). So, Omame et al. built a model by dividing the population into eight subpopulations, namely susceptible (S), susceptible to comorbidity (S_c), individuals infected with COVID-19 without comorbidities (I), isolation and hospitalization for individuals infected with COVID-19 without comorbidity (H), recovered from COVID-19 but without comorbidity (R), infected with COVID-19 and comorbidity (I_c), isolation and hospitalization for those infected with COVID-19 and comorbidity (H_c), and recovered from COVID-19 but with comorbidity (R_c). In another study, Jia et al. [24] by incorporating subpopulations of isolation (H) and quarantine (Q), the model provided divides the population into seven subpopulations, namely S , E , I , A , Q , H , and R . The model is also based on the most recent data from the WHO, indicating that susceptible individuals must first be quarantined to stop the further spread. Research on COVID-19 was also conducted by Prathumwan et al. [25] by adding quarantine subpopulations (Q) and isolation (H) as well so that the model constructed has six subpopulations, namely S , E , I , Q , H , and R . The mathematical model that has been formed needs control to reduce the number of COVID-19 infections. Researchers discussing control issues include Deressa and Duress [26], Olaniyi et al. [27], and Das et al. [22]. Deressa and Duress provide three controls, namely public education, protecting yourself from COVID-19 infection (such as wearing masks, washing hands, and maintaining distance), and treating individuals infected with COVID-19 in hospitals. In comparison, Olaniyi et al. provide two controls, public education and individual care management in hospitals. Other researchers, Das et al. [22], provide two controls to reduce the number of infected with comorbidity and without comorbidity, namely the control other than using drugs and the vaccination process. There are many studies related to COVID-19 besides those mentioned above, see for example the following literature studies [28–54].

By combining the research of Das et al. [22], Jia et al. [24], and Prathumwan et al. [25], the COVID-19 model will be constructed in this study. The discussion is divided into the following sections: The model formulation is presented in Section 2 followed by model validation and mathematical analysis in Section 3. A numerical simulation of the model without control is given in Section 4. Section 5 presents the model with controls and its simulation is given in Section 6. The last discussion on cost evaluation is presented in Section 7. The study is concluded with some key points in Section 8.

2. Model formulation

We consider the new COVID-19 model with eight subpopulations, as shown in the compartment diagram in Figure 1.

Based on the compartmental diagram in Figure 1 and the model assumptions, we have the following system of differential equations:

$$\begin{aligned}
 \frac{dS}{dt} &= \pi - \frac{\beta_1 SI}{N} - \frac{\beta_2 SC}{N} - q_1 S - \mu S, \\
 \frac{dE}{dt} &= \frac{\beta_1 SI}{N} + \frac{\beta_2 SC}{N} - \alpha E - \mu E, \\
 \frac{dI}{dt} &= \xi \alpha E - h_1 I - r_1 I - d_1 I - \mu I, \\
 \frac{dC}{dt} &= (1 - \xi) \alpha E - h_2 C - r_2 C - d_2 C - \mu C, \\
 \frac{dQ}{dt} &= q_1 S - \frac{\rho_1 \beta_1 QI}{N} - \frac{\rho_2 \beta_2 QC}{N} - r_3 Q - \mu Q, \\
 \frac{dH}{dt} &= \theta h_1 I + \delta h_2 C + \frac{p \rho_1 \beta_1 QI}{N} + \frac{q \rho_2 \beta_2 QC}{N} \\
 &\quad - r_4 H - d_3 H - \mu H, \\
 \frac{dJ}{dt} &= (1 - \theta) h_1 I + (1 - \delta) h_2 C \\
 &\quad + \frac{(1 - p) \rho_1 \beta_1 QI}{N} + \frac{(1 - q) \rho_2 \beta_2 QC}{N} - r_5 J - d_4 J - \mu J, \\
 \frac{dR}{dt} &= r_1 I + r_2 C + r_3 Q + r_4 H + r_5 J - \mu R.
 \end{aligned}
 \tag{1}$$

In this model, the COVID-19 model is divided into susceptible (S), exposed (E), infected without comorbidity (I), infected with comorbidity (C), isolated (Q), treatment isolated (H), isolated without treatment (J), and recovered (R). Susceptible subpopulation increases with the recruitment or birth rate denoted by π and can be infected due to contact with infected individuals without comorbidity and with comorbidity denoted by β_1 and β_2 , respectively. Susceptible individuals who are quarantined are denoted by q_1 and cannot be returned to being susceptible due to the effects of public anxiety, which make some assumptions or opinions that susceptible individuals need to be quarantined, so that if quarantine is successful, then recovery is denoted by r_3 and if not successful due to contact with infected individuals without comorbidity and with comorbidity, showing symptoms of being infected, then isolation is denoted by ρ_1 and ρ_2 , respectively. Furthermore, p and q are the proportion of changes from quarantine to isolation. The progression from exposed to infection is denoted α , and ξ is the proportion of change from exposed to infection without comorbidity. From the infected subpopulation without comorbidity and with comorbidity, isolation is denoted by h_1 and h_2 . The parameters r_1, r_2, r_3 , and r_4 indicate the recovery rate of the subpopulations infected without comorbidity, infected with comorbidity, quarantine, isolated with treatment, and isolated without treatment. Furthermore, deaths from each

subpopulation are denoted by μ and deaths from COVID-19 in subpopulations I, C, H , and J are denoted by d_1, d_2, d_3 , and d_4 .

3. Mathematical analysis

3.1. Model validation

We calibrate our model (Equation 1) using cumulatively confirmed COVID-19 cases for Indonesia. We have retrieved COVID-19 case data from the Republic of Indonesia Task Force (SATGAS) situation report for the period 1 November 2020 to 19 May 2021 [9]. The parameter fitting uses the *lsqcurvefit* command, and the value of $MAPE = 0.026022$ is obtained. The results of the fitting parameters seem to match the infection case data as shown in Figure 2, and new parameter values are obtained according to conditions in Indonesia as follows in Table 1.

3.2. Positivity and boundedness of solutions

The change in the total population is given by

$$\begin{aligned}
 \frac{dN}{dt} &= \frac{dS}{dt} + \frac{dE}{dt} + \frac{dI}{dt} + \frac{dC}{dt} + \frac{dQ}{dt} + \frac{dH}{dt} + \frac{dJ}{dt} + \frac{dR}{dt}, \\
 &= \pi - \mu N - d_1 I - d_2 C - d_3 H - d_4 J, \\
 &\leq \pi - \mu N,
 \end{aligned}$$

whose solutions give

$$N(t) \leq \frac{\pi}{\mu} + \left(N(0) - \frac{\pi}{\mu} \right) e^{-\mu t}.$$

Consequently as $t \rightarrow \infty$, then $\lim_{t \rightarrow \infty} N(t) \leq \frac{\pi}{\mu}$. So, we can conclude that N is boundedness to $N(t) \leq \frac{\pi}{\mu}$.

Considering the above solutions, we have that the model has a boundedness solution which is contained in a feasible region Ω , where

$$\Omega = \left\{ (S, E, I, C, Q, H, J, R) \mid N(t) \leq \frac{\pi}{\mu} \right\}.$$

Next, we show the positivity of solving the Equation (1) system by following Riyapan et al. [42] and Roīs et al. [46], as follows:

Theorem 1. Let S, E, I, C, Q, H, J , and R be the system solutions (Equation 1). If $S(0) \geq 0, E(0) \geq 0, I(0) \geq 0, C(0) \geq 0, Q(0) \geq 0, H(0) \geq 0, J(0) \geq 0$, and $R(0) \geq 0$, then all solutions are positive for every $t \geq 0$.

Proof. 1. Take the first equation of the system (Equation 1) as follows:

$$\frac{dS}{dt} = \pi - \frac{\beta_1 SI}{N} - \frac{\beta_2 SC}{N} - q_1 S - \mu S.$$

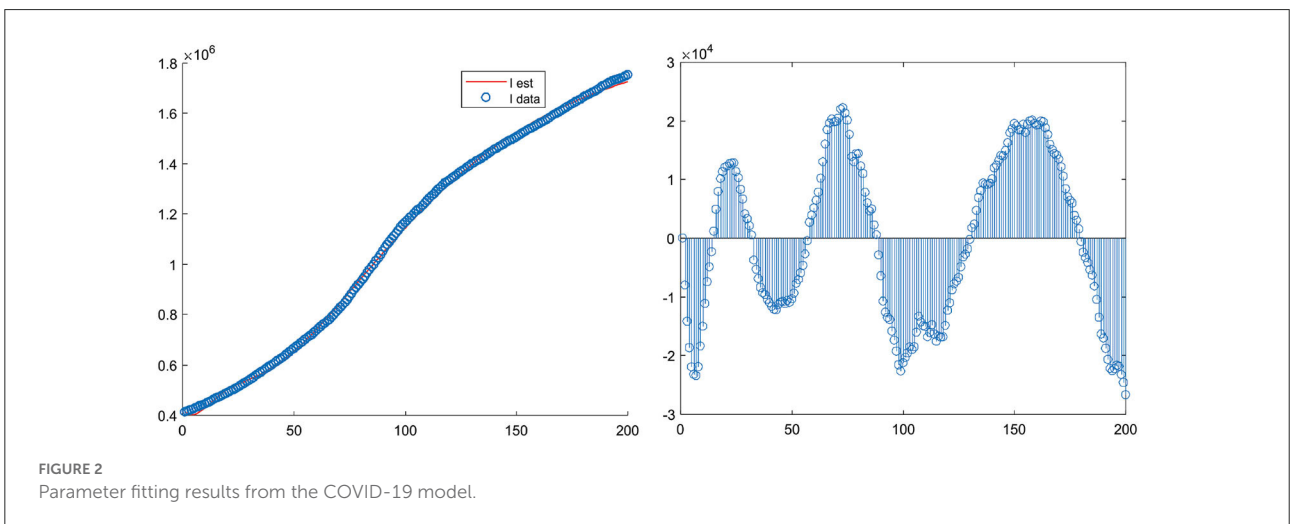
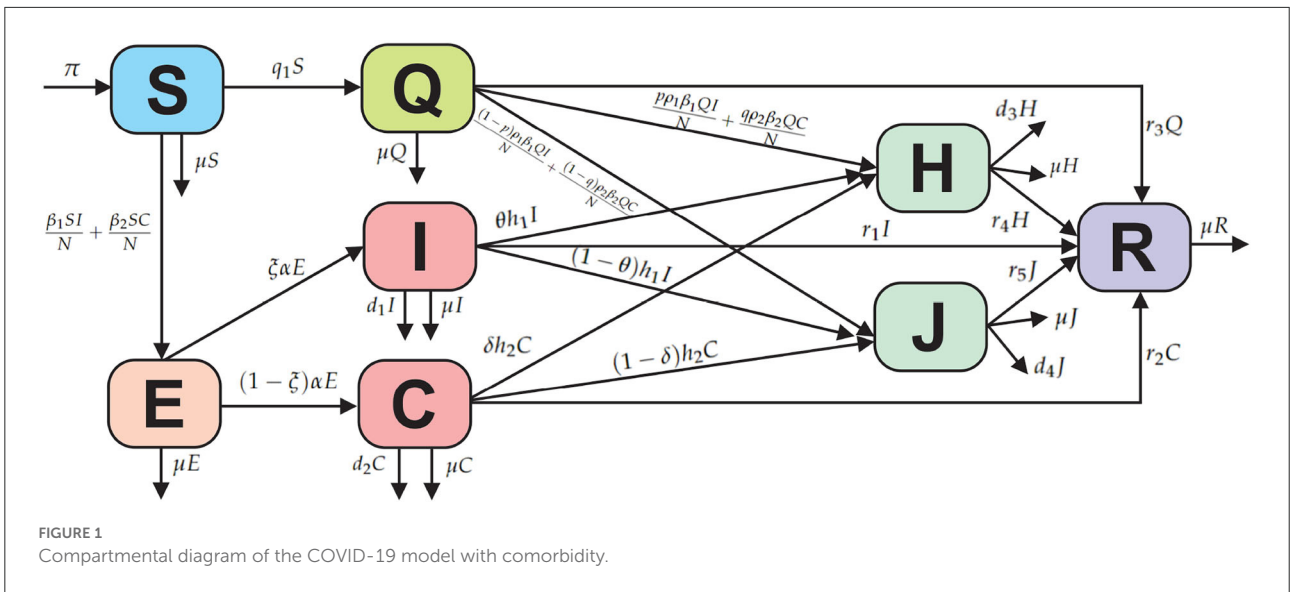


TABLE 1 Parameter values according to the fitting of the infected cases of COVID-19 in Indonesia.

Parameter	Value	Parameter	Value	Parameter	Value
π	3783175.865	r_5	0.088554	δ	0.00059843
β_1	0.65799	h_1	0.007884	p	0.090862
β_2	0.79664	h_2	0.00034162	q	0.28312
q_1	0.16574	ρ_1	0.99779	d_1	0.00086579
r_1	0.0068295	ρ_2	0.9533	d_2	0.022871
r_2	0.0025349	α	0.25098	d_3	0.36203
r_3	0.030397	ξ	0.022219	d_4	0.76233
r_4	0.31851	θ	5.812×10^{-5}	μ	0.0138

Let $\eta = \frac{\beta_1 I}{N} + \frac{\beta_2 C}{N}$.

$$\begin{aligned} \frac{dS}{dt} &= \pi - S(\eta + q_1 + \mu), \\ \frac{dS}{dt} + S(\eta + q_1 + \mu) &= \pi, \\ \frac{d\left(e^{(q_1+\mu)t+\int_0^t \eta ds} S(t)\right)}{dt} &= \pi e^{(q_1+\mu)t+\int_0^t \eta ds}, \end{aligned} \tag{2}$$

then a homogeneous solution is obtained

$$\begin{aligned} \frac{d\left(e^{(q_1+\mu)t+\int_0^t \eta ds} S(t)\right)}{dt} &= 0, \\ S(t) &= ke^{-(q_1+\mu)t-\int_0^t \eta ds}. \end{aligned}$$

Thus, let us assume that the solution is non-homogeneous

$$S(t) = ke^{-(q_1+\mu)t-\int_0^t \eta ds}. \tag{3}$$

Next, substituting the Equation (3) into the Equation (2) to get

$$\begin{aligned} \frac{dk(t)}{dt} &= \pi e^{(q_1+\mu)t+\int_0^t \eta ds}, \\ k(t) &= \int_0^t \pi e^{(q_1+\mu)y+\int_0^y \eta dx} dy + K. \end{aligned} \tag{4}$$

The Equation (4) is substituted into the Equation (3), we get

$$\begin{aligned} S(t) &= \int_0^t \pi e^{(q_1+\mu)y+\int_0^y \eta dx} dy \times e^{-(q_1+\mu)t-\int_0^t \eta ds} \\ &+ S(0)e^{-(q_1+\mu)t-\int_0^t \eta ds}. \end{aligned}$$

So, $S(t)$ is positive for $t \geq 0$.

2. Take the fifth equation of the system (Equation 1) as follows:

$$\frac{dQ}{dt} = q_1 S - \frac{\rho_1 \beta_1 QI}{N} - \frac{\rho_2 \beta_2 QC}{N} - r_3 Q - \mu Q.$$

Let $\omega = \frac{\rho_1 \beta_1 I}{N} + \frac{\rho_2 \beta_2 C}{N}$.

$$\begin{aligned} \frac{dQ}{dt} &= q_1 S - Q(\omega + r_3 + \mu), \\ \frac{dQ}{dt} + Q(\omega + r_3 + \mu) &= q_1 S, \\ \frac{d\left(e^{(r_3+\mu)t+\int_0^t \omega ds} Q(t)\right)}{dt} &= q_1 S e^{(r_3+\mu)t+\int_0^t \omega ds}, \end{aligned} \tag{5}$$

then a homogeneous solution is obtained

$$\begin{aligned} \frac{d\left(e^{(r_3+\mu)t+\int_0^t \omega ds} Q(t)\right)}{dt} &= 0, \\ Q(t) &= ke^{-(r_3+\mu)t-\int_0^t \omega ds}. \end{aligned}$$

Thus, let us assume that the solution is non-homogeneous

$$Q(t) = ke^{-(r_3+\mu)t-\int_0^t \omega ds}. \tag{6}$$

Next, substituting the Equation (6) into the Equation (5) to get

$$\begin{aligned} \frac{dk(t)}{dt} &= q_1 S e^{(r_3+\mu)t+\int_0^t \omega ds}, \\ k(t) &= \int_0^t q_1 S e^{(r_3+\mu)y+\int_0^y \omega dx} dy + K. \end{aligned} \tag{7}$$

The the Equation (7) is substituted into the Equation (6), we get

$$\begin{aligned} Q(t) &= \int_0^t q_1 S e^{(r_3+\mu)y+\int_0^y \omega dx} dy \times e^{-(r_3+\mu)t-\int_0^t \omega ds} \\ &+ Q(0)e^{-(r_3+\mu)t-\int_0^t \omega ds}. \end{aligned}$$

So, $Q(t)$ is positive for $t \geq 0$.

3. Take the second equation of the system (Equation 1) as follows:

$$\frac{dE}{dt} = \frac{\beta_1 SI}{N} + \frac{\beta_2 SC}{N} - \alpha E - \mu E \geq -\alpha E - \mu E,$$

or

$$\begin{aligned} \frac{dE(t)}{dt} &\geq -E(\alpha + \mu), \\ \int \frac{dE(t)}{E} &\geq \int -(\alpha + \mu) dt, \\ E(t) &\geq e^{-(\alpha+\mu)t+k}, \\ E(t) &\geq E(0) e^{-(\alpha+\mu)t}. \end{aligned}$$

Thus, $E(t)$ is positive for $t \geq 0$. Furthermore, in the same way as proof number 3, $I(t)$, $C(t)$, $H(t)$, $J(t)$, and $R(t)$ can be shown respectively to be positive. \square

3.3. Equilibrium point and basic reproduction number

The equilibrium point of the system (Equation 1) is obtained by setting the right-hand side to zeros. Therefore, the first equilibrium point is obtained, namely the disease-free equilibrium point, as follows:

$$\begin{aligned} X^0 &= \left(S^0, E^0, I^0, C^0, Q^0, H^0, J^0, R^0 \right) \\ &= \left(\frac{\pi}{a_1}, 0, 0, 0, \frac{\pi q_1}{a_1 a_5}, 0, 0, \frac{\pi q_1 r_3}{a_1 a_5 \mu} \right). \end{aligned}$$

Where $a_1 = q_1 + \mu$ and $a_5 = r_3 + \mu$.

Furthermore, the basic reproduction number, denoted by R_0 , is obtained using the next-generation matrix method

[55, 56]. The constituent components of the next-generation matrix method only consist of infected subpopulation groups, namely:

$$f = \begin{bmatrix} \frac{\beta_1 SI}{N} + \frac{\beta_2 SC}{N} \\ 0 \\ 0 \end{bmatrix}, \text{ and } v = \begin{bmatrix} a_2 E \\ -\xi \alpha E + a_3 I \\ -(1 - \xi) \alpha E + a_4 C \end{bmatrix}.$$

The partial derivative evaluated at X^0 gives

$$F(X^0) = \begin{bmatrix} 0 & \frac{\beta_1 a_5 \mu}{(a_5 \mu + q_1 \mu + q_1 r_3)} & \frac{\beta_2 a_5 \mu}{(a_5 \mu + q_1 \mu + q_1 r_3)} \\ 0 & 0 & 0 \\ 0 & 0 & 0 \end{bmatrix}$$

$$\text{and } V(X^0) = \begin{bmatrix} a_2 & 0 & 0 \\ -\xi \alpha & a_3 & 0 \\ -(1 - \xi) \alpha & 0 & a_4 \end{bmatrix}.$$

The inverse of the $V(X^0)$ matrix is

$$V^{-1} = \begin{bmatrix} \frac{1}{a_2} & 0 & 0 \\ \frac{\xi \alpha}{a_2 a_3} & \frac{1}{a_3} & 0 \\ \frac{(1 - \xi) \alpha}{a_2 a_4} & 0 & \frac{1}{a_4} \end{bmatrix}.$$

Based on the $F(X^0)$ and $V^{-1}(X^0)$ matrices, the next-generation matrix FV^{-1} can be formed so that we can obtain

$$FV^{-1} = \begin{bmatrix} \frac{\beta_1 a_5 \mu \xi \alpha}{a_2 a_3 (a_5 \mu + q_1 \mu + q_1 r_3)} + \frac{\beta_2 a_5 \mu \alpha (1 - \xi)}{a_2 a_4 (a_5 \mu + q_1 \mu + q_1 r_3)} & \frac{\beta_1 a_5 \mu}{a_3 (a_5 \mu + q_1 \mu + q_1 r_3)} & \frac{\beta_1 a_5 \mu}{a_4 (a_5 \mu + q_1 \mu + q_1 r_3)} \\ 0 & 0 & 0 \\ 0 & 0 & 0 \end{bmatrix}.$$

So, the basic reproduction number is obtained based on the eigenvalues of the FV^{-1} matrix as follows:

$$R_0 = \rho(M) = \frac{a_5 \mu \alpha (\beta_1 \xi a_4 + \beta_2 a_3 (1 - \xi))}{a_2 a_3 a_4 (a_5 \mu + q_1 \mu + q_1 r_3)}.$$

$$J = \begin{bmatrix} B_1 - B_2 - a_1 & B_1 & B_1 - \frac{\beta_1 S}{N} & B_1 - \frac{\beta_2 S}{N} & B_1 & B_1 & B_1 & B_1 \\ B_2 - B_1 & -B_2 - a_2 & \frac{\beta_1 S}{N} - B_1 & \frac{\beta_2 S}{N} - B_1 & -B_1 & -B_1 & -B_1 & -B_1 \\ 0 & \xi \alpha & -a_3 & 0 & 0 & 0 & 0 & 0 \\ 0 & (1 - \xi) \alpha & 0 & -a_4 & 0 & 0 & 0 & 0 \\ q_1 + B_3 & B_3 & B_3 - \frac{\rho_1 \beta_1 Q}{N} & B_3 - \frac{\rho_2 \beta_2 Q}{N} & B_3 - B_4 - a_5 & B_3 & B_3 & B_3 \\ -B_5 & -B_5 & B_6 - B_5 & B_7 - B_5 & B_8 - B_5 & -B_5 - a_6 & -B_5 & -B_5 \\ -B_9 & -B_9 & B_{10} - B_9 & B_{11} - B_9 & B_{12} - B_9 & -B_9 & -B_9 - a_7 & -B_9 \\ 0 & 0 & r_1 & r_2 & r_3 & r_4 & r_5 & -\mu \end{bmatrix} \tag{8}$$

Next, the second equilibrium point is obtained, namely the endemic equilibrium point X^* =

$(S^*, E^*, I^*, C^*, Q^*, H^*, J^*, R^*)$ with

$$\begin{aligned} S^* &= \frac{\pi a_5}{A_1 R_0}, \\ E^* &= \frac{\pi}{a_2 R_0} (R_0 - 1), \\ I^* &= \frac{\pi \xi \alpha}{a_2 a_3 R_0} (R_0 - 1), \\ C^* &= \frac{(1 - \xi) \pi \alpha}{a_2 a_4 R_0} (R_0 - 1), \\ Q^* &= \frac{a_2 a_3 a_4 a_5 q_1 \pi}{A_3}, \\ H^* &= (R_0 - 1) A_4, \\ J^* &= (R_0 - 1) A_5, \\ R^* &= (R_0 - 1) A_6 + \frac{r_3 a_2 a_3 a_4 a_5 q_1 \pi}{\mu A_3}, \end{aligned}$$

with $A_1 = a_5 \mu + \mu q_1 + q_1 r_3$, $A_2 = \rho_1 \beta_1 a_4 \mu \alpha \xi + \rho_2 \beta_2 a_3 \mu \alpha (1 - \xi)$, $A_3 = A_1 A_2 (R_0 - 1) + a_2 a_3 a_4 a_5 A_1 R_0$, $A_4 = \frac{\pi \alpha}{a_6 R_0} \left(\frac{\theta h_1 \xi}{a_2 a_3} + \frac{\delta h_2 (1 - \xi)}{a_2 a_4} + \frac{p \rho_1 \beta_1 q_1 a_4 a_5 \mu \xi}{A_3} + \frac{q \rho_2 \beta_2 q_1 a_3 a_5 \mu (1 - \xi)}{A_3} \right)$, $A_5 = \frac{\pi \alpha}{a_7 R_0} \left(\frac{(1 - \theta) h_1 \xi}{a_2 a_3} + \frac{(1 - \delta) h_2 (1 - \xi)}{a_2 a_4} + \frac{(1 - p) \rho_1 \beta_1 \mu \xi a_4 a_5 q_1}{A_3} + \frac{(1 - q) \rho_2 \beta_2 \mu a_3 a_5 q_1 (1 - \xi)}{A_3} \right)$, and $A_6 = \frac{r_1 \pi \alpha \xi}{\mu a_2 a_3 R_0} + \frac{r_2 \pi \alpha (1 - \xi)}{\mu a_2 a_4 R_0} + \frac{r_4 A_4}{\mu} + \frac{r_5 A_5}{\mu}$.

The existence of the endemic equilibrium point X^* depends on the value of R_0 . If the value of $R_0 < 1$ is taken, then the endemic equilibrium point X^* does not exist because it is clear that E^* , I^* , C^* , H^* , and J^* are obtained negative. If $R_0 = 1$, then we get the equilibrium point $X^* = X^0$, which causes the equilibrium point X^* not to exist. Furthermore, if $R_0 > 1$, then we get S^* , E^* , I^* , C^* , Q^* , H^* , J^* , and R^* are positive and the endemic equilibrium point X^* exists.

3.4. Local stability

The local stability of the equilibrium point is obtained by linearizing system (Equation 1), which yields the following jacobian matrix below:

$$\text{With } B_1 = \frac{\beta_1 SI}{N^2} + \frac{\beta_2 SC}{N^2}, B_2 = \frac{\beta_1 I}{N} + \frac{\beta_2 C}{N}, B_3 = \frac{\rho_1 \beta_1 QI}{N^2} + \frac{\rho_2 \beta_2 QC}{N^2}, B_4 = \frac{\rho_1 \beta_1 I}{N} + \frac{\rho_2 \beta_2 C}{N}, B_5 = \frac{p \rho_1 \beta_1 QI}{N^2} + \frac{q \rho_2 \beta_2 QC}{N^2}, B_6 =$$

$$\theta h_1 + \frac{p\rho_1\beta_1Q}{N}, B_7 = \delta h_2 + \frac{q\rho_2\beta_2Q}{N}, B_8 = \frac{p\rho_1\beta_1I}{N} + \frac{q\rho_2\beta_2C}{N}, B_9 = \frac{(1-p)\rho_1\beta_1QI}{N^2} + \frac{(1-q)\rho_2\beta_2QC}{N^2}, B_{10} = (1-\theta)h_1 + \frac{(1-p)\rho_1\beta_1Q}{N}, B_{11} = (1-\delta)h_2 + \frac{(1-q)\rho_2\beta_2Q}{N}, \text{ and } B_{12} = \frac{(1-p)\rho_1\beta_1I}{N} + \frac{(1-q)\rho_2\beta_2C}{N}.$$

3.4.1. Local stability of disease-free equilibrium point

Evaluating (8) at X^0 yields

$$J(X^0) = \begin{bmatrix} -a_1 & 0 & -\beta_1C_1 & -\beta_2C_1 & 0 & 0 & 0 & 0 \\ 0 & -a_2 & \beta_1C_1 & \beta_2C_1 & 0 & 0 & 0 & 0 \\ 0 & \xi\alpha & -a_3 & 0 & 0 & 0 & 0 & 0 \\ 0 & (1-\xi)\alpha & 0 & -a_4 & 0 & 0 & 0 & 0 \\ q_1 & 0 & -\rho_1\beta_1C_2 & -\rho_2\beta_2C_2 & -a_5 & 0 & 0 & 0 \\ 0 & 0 & \theta h_1 + p\rho_1\beta_1C_2 & \delta h_2 + q\rho_2\beta_2C_2 & 0 & -a_6 & 0 & 0 \\ 0 & 0 & (1-\theta)h_1 + (1-p)\rho_1\beta_1C_2 & (1-\delta)h_2 + (1-q)\rho_2\beta_2C_2 & 0 & 0 & -a_7 & 0 \\ 0 & 0 & r_1 & r_2 & r_3 & r_4 & r_5 & -\mu \end{bmatrix},$$

With $C_1 = \frac{a_5\mu}{(a_5+q_1)\mu+q_1r_3}$ and $C_2 = \frac{q_1\mu}{(a_5+q_1)\mu+q_1r_3}$. The characteristic equation for the $|J(X^0) - \lambda I| = 0$ is as follows:

$$\begin{vmatrix} (-a_1 - \lambda) & 0 & 0 & 0 & 0 \\ 0 & (-a_2 - \lambda) & \beta_1C_1 & \beta_2C_1 & 0 \\ 0 & \xi\alpha & (-a_3 - \lambda) & 0 & 0 \\ 0 & (1-\xi)\alpha & 0 & (-a_4 - \lambda) & 0 \\ 0 & 0 & 0 & 0 & (-a_5 - \lambda) \\ 0 & 0 & \theta h_1 + p\rho_1\beta_1C_2 & \delta h_2 + q\rho_2\beta_2C_2 & 0 \\ 0 & 0 & (1-\theta)h_1 + (1-p)\rho_1\beta_1C_2 & (1-\delta)h_2 + (1-q)\rho_2\beta_2C_2 & 0 \\ 0 & 0 & r_1 & r_2 & r_3 & r_4 & r_5 & (-\mu - \lambda) \end{vmatrix} = 0. \tag{9}$$

Based on the Equation (9), we obtain the eigenvalues $\lambda_1 = \lambda_2 = \lambda_3 = \lambda_4 = \lambda_5 < 0$. Therefore, the stability of the disease-free equilibrium point depends on

$$M_1 = \begin{vmatrix} -a_2 - \lambda & \beta_1C_1 & \beta_2C_1 \\ \xi\alpha & -a_3 - \lambda & 0 \\ (1-\xi)\alpha & 0 & -a_4 - \lambda \end{vmatrix}. \tag{10}$$

From the Equation (10), we obtain the following characteristic equation:

$$\lambda^3 + k_1\lambda^2 + k_2\lambda + k_3 = 0, \tag{11}$$

with

$$J(X^*) = \begin{bmatrix} B_1 - B_{13} & B_1 & B_1 - \frac{\beta_1S^*}{N} & B_1 - \frac{\beta_2S^*}{N} & B_1 & B_1 & B_1 & B_1 \\ B_2 - B_1 & -B_{14} & \frac{\beta_1S^*}{N} - B_1 & \frac{\beta_2S^*}{N} - B_1 & -B_1 & -B_1 & -B_1 & -B_1 \\ 0 & \xi\alpha & -a_3 & 0 & 0 & 0 & 0 & 0 \\ 0 & (1-\xi)\alpha & 0 & -a_4 & 0 & 0 & 0 & 0 \\ q_1 + B_3 & B_3 & B_3 - \frac{\rho_1\beta_1Q^*}{N} & B_3 - \frac{\rho_2\beta_2Q^*}{N} & B_3 - B_{15} & B_3 & B_3 & B_3 \\ -B_5 & -B_5 & B_6 - B_5 & B_7 - B_5 & B_8 - B_5 & -B_{16} & -B_5 & -B_5 \\ -B_9 & -B_9 & B_{10} - B_9 & B_{11} - B_9 & B_{12} - B_9 & -B_9 & -B_{17} & -B_9 \\ 0 & 0 & r_1 & r_2 & r_3 & r_4 & r_5 & -\mu \end{bmatrix},$$

$$k_1 = a_2 + a_3 + a_4, \\ k_2 = a_2a_3(1-R_0) + a_2a_4(1-R_0) + a_3a_4 + \frac{a_4\beta_1\alpha C_1\xi}{a_3} + \frac{a_3\beta_2\alpha C_1(1-\xi)}{a_4}, \text{ and} \\ k_3 = a_2a_3a_4(1-R_0).$$

In the Equation (11), it is clear that $k_1 > 0$, and if $R_0 < 1$, then $k_2 > 0$ and $k_3 > 0$. Therefore, the stability property of the equilibrium point X^0 is established using the Routh–Hurwitz criterion. Furthermore, the equilibrium point X^0 is asymptotically stable if and only if it satisfies the following criteria:

1. $k_1 > 0$,
2. $k_3 > 0$, and
3. $k_1k_2 - k_3 > 0$.

Criteria Equations (1) and (2) have been met so that the disease-free equilibrium point X^0 is locally asymptotically stable if it meets $k_1k_2 - k_3 > 0$ where

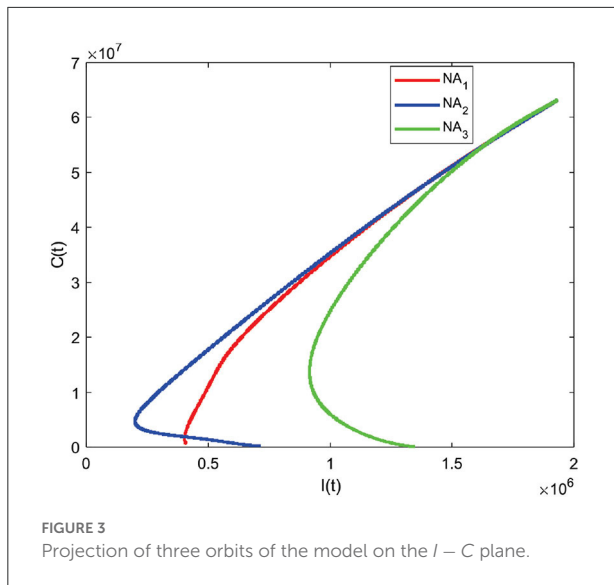
$$k_1k_2 - k_3 > 0, \\ (a_2 + a_3 + a_4) \left(a_2a_4(1-R_0) + a_3a_4 + \frac{a_4\beta_1\alpha C_1\xi}{a_3} + \frac{a_3\beta_2\alpha C_1(1-\xi)}{a_4} \right) + a_2^2a_3(1-R_0) + a_2a_3^2(1-R_0) > 0.$$

It is clear that the Routh–Hurwitz criteria are satisfied; thus, the roots of the characteristic Equation (11) have negative real parts. Therefore, the disease-free equilibrium point is asymptotically locally stable if $R_0 < 1$.

3.4.2. Local stability of the endemic equilibrium point

Evaluating (8) at X^* yields

$$\text{With } B_1 = \frac{\beta_1S^*I^*}{N^2} + \frac{\beta_2S^*C^*}{N^2}, B_2 = \frac{\beta_1I^*}{N} + \frac{\beta_2C^*}{N}, \\ B_3 = \frac{\rho_1\beta_1Q^*I^*}{N^2} + \frac{\rho_2\beta_2Q^*C^*}{N^2}, B_4 = \frac{\rho_1\beta_1I^*}{N} + \frac{\rho_2\beta_2C^*}{N}, B_5 = \frac{p\rho_1\beta_1Q^*I^*}{N^2} + \frac{q\rho_2\beta_2Q^*C^*}{N^2}, B_6 = \theta h_1 + \frac{p\rho_1\beta_1Q^*}{N}, B_7 = \delta h_2 + \frac{q\rho_2\beta_2Q^*}{N}, B_8 = \frac{p\rho_1\beta_1I^*}{N} + \frac{q\rho_2\beta_2C^*}{N}, B_9 = \frac{(1-p)\rho_1\beta_1Q^*I^*}{N^2} +$$



$$\begin{aligned} \frac{(1-q)\rho_2\beta_2Q^*C^*}{N^2}, B_{10} &= (1-\theta)h_1 + \frac{(1-p)\rho_1\beta_1Q^*}{N}, B_{11} = \\ (1-\delta)h_2 + \frac{(1-q)\rho_2\beta_2Q^*}{N}, B_{12} &= \frac{(1-p)\rho_1\beta_1I}{N} + \frac{(1-q)\rho_2\beta_2C}{N}, \\ B_{13} &= B_2 + a_1, B_{14} = B_2 + a_2, B_{15} = B_4 + a_5, B_{16} = B_5 + a_6, \\ \text{and } B_{17} &= B_9 + a_7. \end{aligned}$$

The characteristic equation of the $|J(X^*) - \lambda I| = 0$ is

$$\lambda^8 + k_1\lambda^7 + k_2\lambda^6 + k_3\lambda^5 + k_4\lambda^4 + k_5\lambda^3 + k_6\lambda^2 + k_7\lambda + k_8 = 0, \tag{12}$$

It is difficult to prove analytically that all eigenvalues of J have negative real parts for $R_0 > 1$. However, from our numerical simulations (case $R_0 > 1$), all eigenvalues have negative real parts.

Figure 3 gives the projection of three orbits of three different initial conditions when $R_0 > 1$ on the $I - C$ plane. The component (I, C) of the equilibrium X^* is not $(0, 0)$. This simulation indicates that the endemic equilibrium X^* is locally asymptotically stable when $R_0 > 1$.

3.5. Global stability analysis

In this study, we prove the global stability of disease-free and endemic equilibrium points by constructing the suitable Lyapunov function and following the theorem from Alligood et al. [57].

3.5.1. Global stability of the disease-free equilibrium point

Theorem 2. Disease-free equilibrium point X^0 is globally asymptotically stable if $R_0 < 1$ and unstable if $R_0 > 1$.

Proof. Defined Lyapunov function

$$L = \kappa_1 E + \kappa_2 I + \kappa_3 C, \tag{13}$$

where

$$\begin{aligned} \kappa_1 &= a_1 a_2 a_3 a_4, \\ \kappa_2 &= \frac{\pi \beta_1 a_2 a_4}{N}, \text{ and} \\ \kappa_3 &= \frac{\pi \beta_2 a_2 a_3}{N}. \end{aligned}$$

The function L needs to be proven to determine whether Lyapunov is strong or weak for X^0 .

$$\begin{aligned} L(\vec{x}^*) &= L(S^0, E^0, I^0, C^0, Q^0, H^0, J^0, R^0), \\ L(\vec{x}^*) &= \kappa_1 E^0 + \kappa_2 I^0 + \kappa_3 C^0 = 0. \end{aligned}$$

It is proven that $L(\vec{x}^*) = 0$. Next,

$$L(\vec{x}) = \kappa_1 E + \kappa_2 I + \kappa_3 C,$$

Because $\forall (S, E, I, C, Q, H, J, R) \neq (S^0, E^0, I^0, C^0, Q^0, H^0, J^0, R^0)$, so it is proved that $L(\vec{x}) > 0$.

Thus, the Equation (13) can be reduced to

$$\begin{aligned} \frac{\partial L}{\partial t} &= \kappa_1 \frac{dE}{dt} + \kappa_2 \frac{dI}{dt} + \kappa_3 \frac{dC}{dt} \\ &= \kappa_1 \left(\frac{\beta_1 SI + \beta_2 SC}{N} - a_2 E \right) \\ &\quad + \kappa_2 (\xi \alpha E - a_3 I) + \kappa_3 ((1 - \xi) \alpha E - a_4 C), \end{aligned}$$

so, we obtain

$$\begin{aligned} &= a_1 a_2 a_3 a_4 \left(\frac{\beta_1 SI + \beta_2 SC}{N} - a_2 E + \frac{\pi \beta_1 a_2 a_4 \xi \alpha E}{a_1 a_2 a_3 a_4 N} \right. \\ &\quad \left. + \frac{\pi \beta_2 a_2 a_3 (1 - \xi) \alpha E}{a_1 a_2 a_3 a_4 N} - \frac{\pi \beta_1 I}{a_1 N} - \frac{\pi \beta_2 C}{a_1 N} \right). \end{aligned}$$

Let $S = \frac{\pi}{a_1}$, so we get

$$\frac{\partial L}{\partial t} = a_1 a_2^2 a_3 a_4 E (R_0 - 1).$$

Based on the description above, it can be concluded that $\frac{\partial L}{\partial t} < 0$ if $R_0 < 1$ and $\frac{\partial L}{\partial t} = 0$ if $E = 0$. Hence, by Lasalle's invariance principle, the disease-free equilibrium point in the spread of COVID-19 (X^0) is globally asymptotically stable if $R_0 < 1$. □

3.5.2. Global stability of the endemic equilibrium point

Theorem 3. If $R_0 > 1$, then the endemic equilibrium point X^* is said to be globally asymptotically stable.

TABLE 2 Stability conditions.

Equilibrium point	Existence requirement	Global stability type	Stability condition
X^0	None	Asymptotically stable	$R_0 < 1$
X^*	$R_0 > 1$	Asymptotically stable	$R_0 > 1$ and strong Lyapunov function

Proof. The Lyapunov function is defined as follows:

$$L = \frac{1}{2} [S_S + E_E + I_I + C_C + Q_Q + H_H + J_J + R_R]^2, \quad (14)$$

Where $S_S = (S - S^*)$, $E_E = (E - E^*)$, $I_I = (I - I^*)$, $C_C = (C - C^*)$, $Q_Q = (Q - Q^*)$, $H_H = (H - H^*)$, $J_J = (J - J^*)$, and $R_R = (R - R^*)$.

The function L needs to be proven to determine whether the Lyapunov function is strong or weak for X^* .

$$L(\vec{x}^*) = L(S^*, E^*, I^*, C^*, Q^*, H^*, J^*, R^*),$$

$$L(\vec{x}^*) = \frac{1}{2} [S_S^* + E_E^* + I_I^* + C_C^* + Q_Q^* + H_H^* + J_J^* + R_R^*]^2 = 0.$$

Where $S_S^* = (S^* - S^*)$, $E_E^* = (E^* - E^*)$, $I_I^* = (I^* - I^*)$, $C_C^* = (C^* - C^*)$, $Q_Q^* = (Q^* - Q^*)$, $H_H^* = (H^* - H^*)$, $J_J^* = (J^* - J^*)$, and $R_R^* = (R^* - R^*)$. It is proven that $L(\vec{x}^*) = 0$.

Next,

$$L(\vec{x}) = \frac{1}{2} [S_S + E_E + I_I + C_C + Q_Q + H_H + J_J + R_R]^2.$$

Because $\forall (S, E, I, C, Q, H, J, R) \neq (S^0, E^0, I^0, C^0, Q^0, H^0, J^0, R^0)$, so that it is proven that $L(\vec{x}) > 0$. Next, we check that the Equation (14) is reduced to

$$\begin{aligned} \frac{\partial L}{\partial t} &= [S_S + E_E + I_I + C_C + Q_Q + H_H + J_J + R_R] \\ &\quad \frac{d}{dt} [S + E + I + C + Q + H + J + R], \\ &= [S_S + E_E + I_I + C_C + Q_Q + H_H + J_J + R_R] \\ &\quad [\pi - \mu(S + E + I + C + Q + H + J + R) \\ &\quad - d_1 I - d_2 C - d_3 H - d_4 J], \end{aligned}$$

Let $\pi = \mu(S^* + E^* + I^* + C^* + Q^* + H^* + J^* + R^*) + d_1 I^* + d_2 C^* + d_3 H^* + d_4 J^*$. So that it gives

$$\begin{aligned} &= [S_S + E_E + I_I + C_C + Q_Q + H_H + J_J + R_R] \\ &\quad \times [-[\mu(S_S + E_E + I_I + C_C + Q_Q + H_H + J_J + R_R) + d_1(I - I^*) \\ &\quad + d_2(C - C^*) + d_3(H - H^*) + d_4(J - J^*)]], \\ &= -[S_S + E_E + I_I + C_C + Q_Q + H_H + J_J + R_R] \\ &\quad \times [\mu(S_S + E_E + I_I + C_C + Q_Q + H_H + J_J + R_R) + d_1(I - I^*) \\ &\quad + d_2(C - C^*) + d_3(H - H^*) + d_4(J - J^*)]. \end{aligned}$$

Based on the description above, it can be concluded that $\frac{\partial L}{\partial t} < 0$ if $R_0 > 1$ and $\frac{\partial L}{\partial t} = 0$ if $S = S^*$, $E = E^*$, $I = I^*$, $C = C^*$, $Q = Q^*$, $H = H^*$, $J = J^*$, and $R = R^*$. Hence, by Lasalle's invariance principle, it means that the endemic equilibrium point in the spread of COVID-19 (X^*) is globally asymptotically stable if $R_0 > 1$. \square

The terms of existence and the type of stability of the equilibrium point of the system of equations are summarized in Table 2.

3.6. Sensitivity analysis

The sensitivity analysis aims to determine the parameters that cause the spread of the COVID-19 virus. The sensitivity index of the basic reproduction number depends on the differentiation of the parameters contained in the basic reproduction number [58, 59]. Sensitivity index R_0 to the parameters is as follows:

$$\begin{aligned} I_\alpha^{R_0} &= \frac{\partial R_0}{\partial \alpha} \frac{\alpha}{R_0} = \frac{\mu}{\alpha + \mu}, \\ I_{\beta_1}^{R_0} &= \frac{\partial R_0}{\partial \beta_1} \frac{\beta_1}{R_0} = \frac{\beta_1 \xi a_4}{\beta_1 \xi a_4 + \beta_2 a_3 (1 - \xi)}, \\ I_{\beta_2}^{R_0} &= \frac{\partial R_0}{\partial \beta_2} \frac{\beta_2}{R_0} = \frac{\beta_2 a_3 (1 - \xi)}{\beta_1 \xi a_4 + \beta_2 a_3 (1 - \xi)}, \\ I_\xi^{R_0} &= \frac{\partial R_0}{\partial \xi} \frac{\xi}{R_0} = \frac{\beta_1 \xi a_4 - \beta_2 \xi a_3}{\beta_1 \xi a_4 + \beta_2 a_3 (1 - \xi)}, \\ I_{q_1}^{R_0} &= \frac{\partial R_0}{\partial q_1} \frac{q_1}{R_0} = -\frac{q_1}{q_1 + \mu}, \\ I_{h_1}^{R_0} &= \frac{\partial R_0}{\partial h_1} \frac{h_1}{R_0} = \frac{a_4 \beta_1 h_1 \xi}{-a_3 (\beta_2 a_3 (1 - \xi) + \beta_1 a_4 \xi)}, \\ I_{r_1}^{R_0} &= \frac{\partial R_0}{\partial r_1} \frac{r_1}{R_0} = \frac{\beta_1 r_1 a_4 \xi}{-a_3 (\beta_2 a_3 (1 - \xi) + \beta_1 a_4 \xi)}, \\ I_{d_1}^{R_0} &= \frac{\partial R_0}{\partial d_1} \frac{d_1}{R_0} = \frac{\beta_1 d_1 a_4 \xi}{-a_3 (\beta_2 a_3 (1 - \xi) + \beta_1 a_4 \xi)}, \\ I_{h_2}^{R_0} &= \frac{\partial R_0}{\partial h_2} \frac{h_2}{R_0} = \frac{\beta_2 h_2 a_3 (1 - \xi)}{-a_4 (\beta_2 a_3 (1 - \xi) + \beta_1 a_4 \xi)}, \\ I_{r_2}^{R_0} &= \frac{\partial R_0}{\partial r_2} \frac{r_2}{R_0} = \frac{\beta_2 r_2 a_3 (1 - \xi)}{-a_4 (\beta_2 a_3 (1 - \xi) + \beta_1 a_4 \xi)}, \\ I_{d_2}^{R_0} &= \frac{\partial R_0}{\partial d_2} \frac{d_2}{R_0} = \frac{\beta_2 r_2 a_3 (1 - \xi)}{-a_4 (\beta_2 a_3 (1 - \xi) + \beta_1 a_4 \xi)}, \end{aligned}$$

TABLE 3 Sensitivity analysis.

No	Parameter	Sensitivity index
1	q_1	-0.9761
2	β_2	0.9754
3	μ	0.5715
4	d_2	-0.5636
5	r_2	-0.0625
6	α	0.0522
7	β_1	0.0246
8	h_2	-0.0084
9	h_1	-0.0066
10	r_1	-0.0057
11	ξ	0.0025
12	d_1	-0.0007

Next, the graph of the solution $R_0 < 1$ is obtained in Figure 4.

The analysis results from 3.4.1, and Theorem 2 are illustrated numerically. Numerical simulations with some initial values show that the graph solution is toward and close to the disease-free equilibrium point X^0 (converging toward the disease-free equilibrium point X_0). Based on the graph, this means that after all this time, no individual has been infected with COVID-19. The numerical results support the analysis that if $R_0 < 1$, then the disease-free equilibrium point X^0 is asymptotically stable locally and globally given different initial values.

We show the stability of the endemic equilibrium point, the parameter values in Table 1 are used, and three different values, so we get $R_0 = 1.47 > 1$. Similarly, the disease-free equilibrium point is obtained

$$X^0 = (21071493, 0, 0, 0, 79018695, 0, 0, 174052991)$$

and the endemic equilibrium point is given as

$$I_\mu^{R_0} = \frac{\partial R_0}{\partial \mu} \frac{\mu}{R_0} = \frac{-\left(\alpha((-2\xi + 2)\beta_2 + 2\beta_1\xi)\mu^5 + a_8(1 - \xi)\beta_2 + \beta_1 a_9 \xi\right)\mu^4 + 2a_{10}\left((1 - \xi)a_3\beta_2 + \beta_1\xi a_4\right)\mu^3}{a_1^2 a_2^2 a_3^2 a_4^2} - \frac{\left(\left((-a_{12})q_1 + a_{11}^2\right)\alpha + a_{11}^2(a_{12} + q_1)(\xi - 1)\beta_2 - \left(\left(a_{11}\right)q_1 - a_{12}^2\right)\alpha - a_{12}^2(a_{11} + q_1)\right)\beta_1\xi\right)\mu^2}{a_1^2 a_2^2 a_3^2 a_4^2} - \frac{2(a_{11}\alpha q_1(\beta_1\xi + \beta_2(1 - \xi))a_{11}\mu + a_{12}\alpha((\xi - 1)a_{11}\beta_2 - \beta_1\xi a_{12})q_1 a_{11})}{a_1^2 a_2^2 a_3^2 a_4^2}$$

With $a_8 = (4d_1 + \alpha + d_2 + h_1 + h_2 + q_1 + 4r_1 + r_2)$, $a_9 = d_1 + \alpha + 4d_2 + h_1 + 4h_2 + q_1 + r_1 + 4r_2$, $a_{10} = (d_1 + \alpha + d_2 + h_1 + h_2 + q_1 + r_1 + r_2)$, $a_{11} = h_1 + r_1 + d_1$, and $a_{12} = h_2 + r_2 + d_2$.

The parameter sensitivity index is shown in Table 3.

From Table 3, we can see that the most sensitive parameters are q_1 and β_2 . A positive index means that if we reduce the parameter by almost 10%, then the value of the basic reproduction number can decrease by 10%.

4. Simulation of the model without control

This section presents a numerical solution of system (1) using the Fourth-order Runge-Kutta method. The parameter values used in this simulation are shown in Table 1 and three different initial values. In this simulation, the stability of the disease-free equilibrium point is shown from the parameter values given in Table 1, except for the parameter $q_1 = 0.56574$, the value is $R_0 = 0.456 < 1$. Based on the value of these parameters, the disease-free equilibrium point is obtained, namely $X^0 = (6527542, 0, 0, 0, 83496205, 0, 0, 183499868)$.

$$X^* = (S^*, E^*, I^*, C^*, Q^*, H^*, J^*, R^*), \\ = (6031017, 10196616, 1933377, 63222893, 2119885, 362896, 798735, 30671327).$$

The solution graph for the case of $R_0 > 1$ is obtained as follows in Figure 5.

The numerical simulation results support the analysis from 3.4.2 and Theorem 3 that some of the initial values given are obtained by the graph of the solution leading to the endemic equilibrium point X^* (converging to the endemic equilibrium point X^*), which means there is a spread of disease due to COVID-19. The numerical simulation results follow the analysis that if $R_0 > 1$, the endemic equilibrium point X^* is asymptotically stable locally and globally with different initial values. Based on the given parameter values, we obtain $R_0 > 1$. This means that there is an outbreak of disease due to COVID-19. Therefore, it is necessary to take control measures to reduce the outbreak.

4.1. Effect parameters

The effect of parameters on R_0 was analyzed using contour plots. We choose two significant parameters, q_1

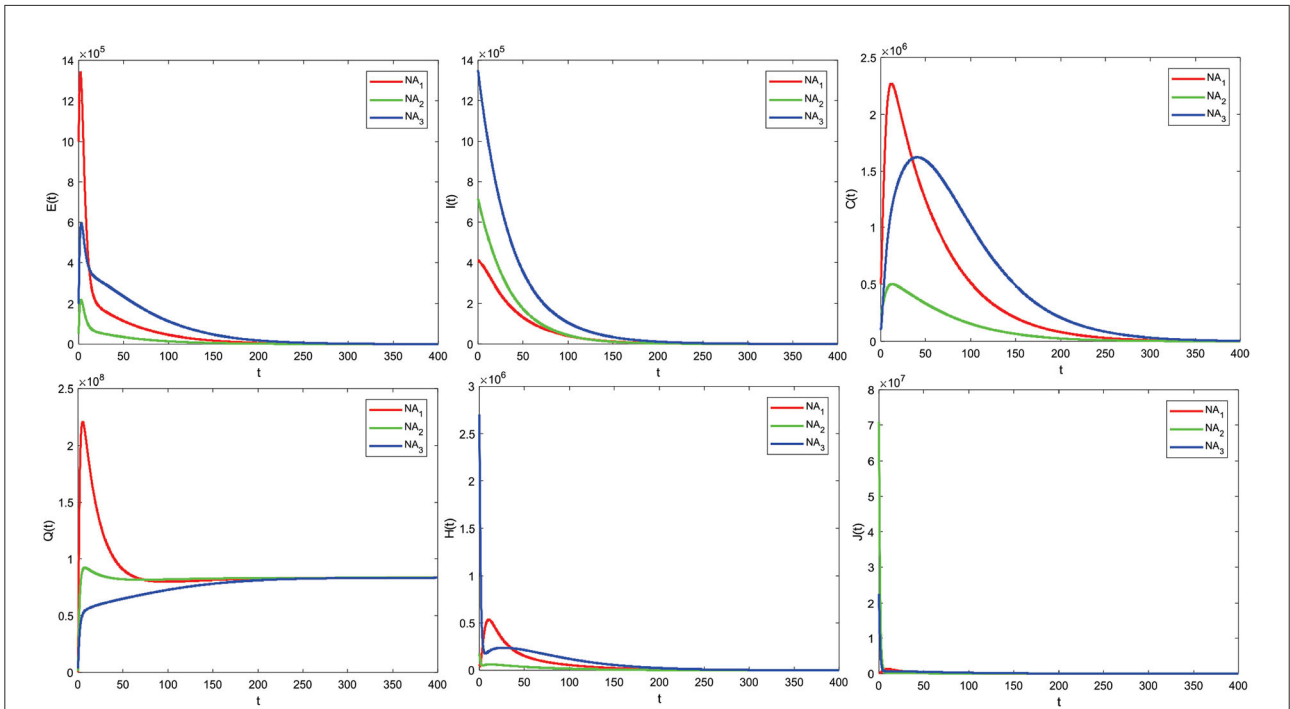


FIGURE 4
COVID-19 model solution graph for $R_0 < 1$.

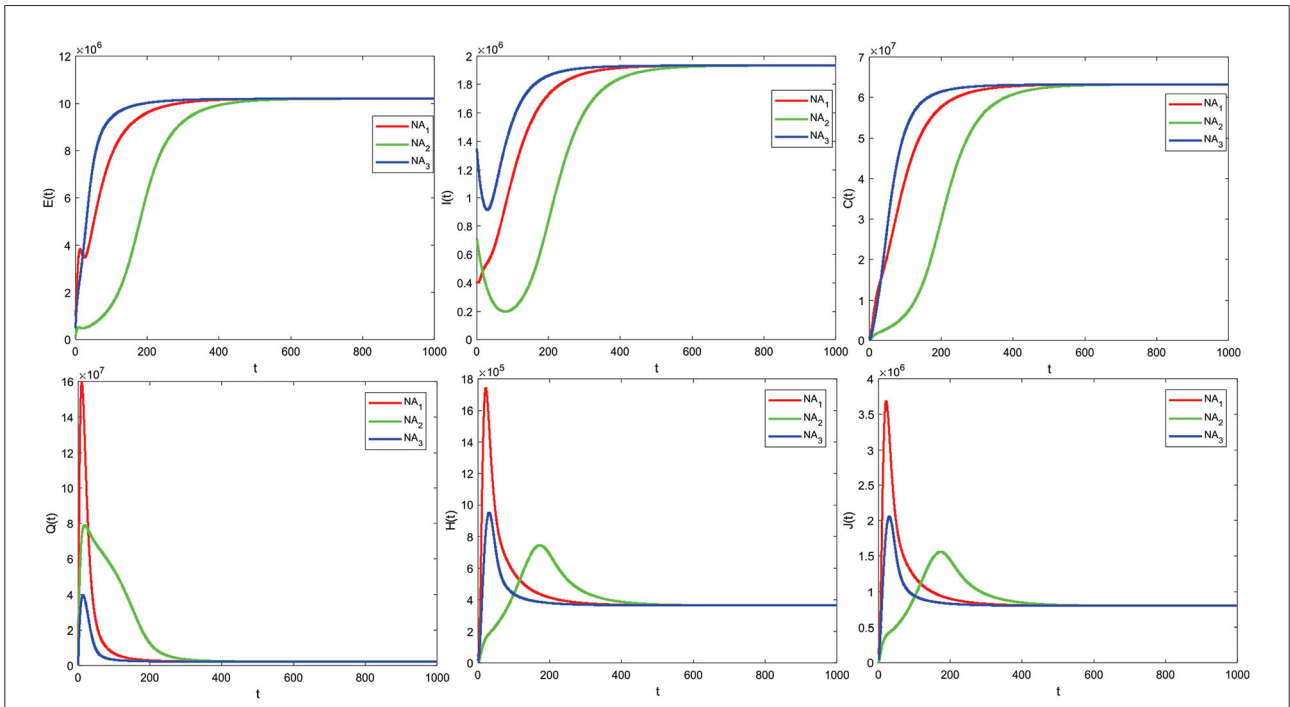


FIGURE 5
The COVID-19 model solution graph for $R_0 > 1$.

and β_2 , and provide a contour plot as a function of R_0 . The impact of some R_0 parameters is further investigated in Figure 6. Figure 6 shows that increasing the parameter q_1 decreases the value of R_0 . This implies that increasing quarantines has the effect of reducing the spread of COVID-19. Meanwhile, an increase in the β_2 parameter resulted in an increase in the R_0 value and implied that an increase in contacts of individuals with comorbidities would increase the spread of COVID-19, especially individuals with comorbidities. Therefore, increasing quarantine and reducing contact with individuals with comorbidities are important.

5. Optimal control problem

5.1. Comorbidity COVID-19 model with optimal control

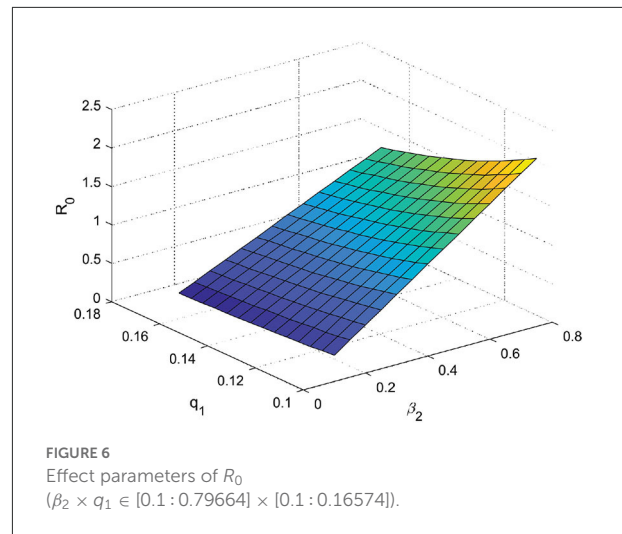
The control variable given to the COVID-19 model consists of preventive measures through education (u_1) and individual treatment efforts for infected (u_2). So the model with control is given as follows:

$$\begin{aligned}
 \frac{dS}{dt} &= \pi - (1 - u_1) \frac{(\beta_1 SI + \beta_2 SC)}{N} - q_1 S - \mu S, \\
 \frac{dE}{dt} &= (1 - u_1) \frac{(\beta_1 SI + \beta_2 SC)}{N} - \alpha E - \mu E, \\
 \frac{dI}{dt} &= \xi \alpha E - (h_1 + u_2) I - r_1 I - d_1 I - \mu I, \\
 \frac{dC}{dt} &= (1 - \xi) \alpha E - (h_2 + u_2) C - r_2 C - d_2 C - \mu C, \\
 \frac{dQ}{dt} &= q_1 S - \frac{\rho_1 \beta_1 QI}{N} - \frac{\rho_2 \beta_2 QC}{N} - r_3 Q - \mu Q, \quad (15) \\
 \frac{dH}{dt} &= (\theta h_1 + u_2) I + \frac{p \rho_1 \beta_1 QI}{N} \\
 &+ \frac{q \rho_2 \beta_2 QC}{N} + (\delta h_2 + u_2) C - r_4 H - d_3 H - \mu H, \\
 \frac{dJ}{dt} &= ((1 - \theta) h_1 + u_2) I \\
 &+ ((1 - \delta) h_2 + u_2) C + \frac{(1 - p) \rho_1 \beta_1 QI}{N} \\
 &+ \frac{(1 - q) \rho_2 \beta_2 QC}{N} - a_7 J, \\
 \frac{dR}{dt} &= r_1 I + r_2 C + r_3 Q + r_4 H + r_5 J - \mu R.
 \end{aligned}$$

The function that minimizes the number of infected cases without comorbidity (I) and the number of infected cases with comorbidity (C) over a time interval $[0, T]$ can be defined as

$$J(u_1, u_2) = \int_0^T \left(I(t) + C(t) + \frac{1}{2} (A_1 u_1^2 + A_2 u_2^2) \right), \quad (16)$$

Where A_1 and A_2 are the relative cost associated with the controls u_1 and u_2 , and T is the final time. The aim of the control



is to minimize the cost function.

$$J(u_1^*, u_2^*) = \min J(u_1, u_2),$$

Subject to the system (Equation 15), where $0 \leq (u_1, u_2) \leq 1$ and $t \in (0, T)$.

5.2. Optimal control analysis

The Hamilton function can be defined as follows:

$$\begin{aligned}
 \mathcal{H} &= I + C + \frac{1}{2} (A_1 u_1^2 + A_2 u_2^2) \\
 &+ \lambda_1 \left(\pi - (1 - u_1) \frac{(\beta_1 SI + \beta_2 SC)}{N} - q_1 S - \mu S \right) \\
 &+ \lambda_2 \left((1 - u_1) \frac{(\beta_1 SI + \beta_2 SC)}{N} - \alpha E - \mu E \right) \\
 &+ \lambda_3 \left(\xi \alpha E - (h_1 + u_2) I - r_1 I - d_1 I - \mu I \right) \\
 &+ \lambda_4 \left((1 - \xi) \alpha E - (h_2 + u_2) C - r_2 C - d_2 C - \mu C \right) \\
 &+ \lambda_5 \left(q_1 S - \frac{\rho_1 \beta_1 QI}{N} - \frac{\rho_2 \beta_2 QC}{N} - r_3 Q - \mu Q \right) \quad (17) \\
 &+ \lambda_6 \left((\theta h_1 + u_2) I + \frac{p \rho_1 \beta_1 QI}{N} \right. \\
 &+ \left. \frac{q \rho_2 \beta_2 QC}{N} + (\delta h_2 + u_2) C - r_4 H - d_3 H - \mu H \right) \\
 &+ \lambda_7 \left(((1 - \theta) h_1 + u_2) I + ((1 - \delta) h_2 + u_2) C \right. \\
 &+ \left. \frac{(1 - p) \rho_1 \beta_1 QI}{N} + \frac{(1 - q) \rho_2 \beta_2 QC}{N} - a_7 J \right) \\
 &+ \lambda_8 (r_1 I + r_2 C + r_3 Q + r_4 H + r_5 J - \mu R).
 \end{aligned}$$

Based on Pontryagin's principle, the Hamilton function will reach an optimal solution if it satisfies the state equation

and the costate equation, and the condition is stationary. The equation state is obtained by deriving the Hamilton function (Equation 17) for each variable costate as Equation (15). Next, the equation costate is the negative value of the derivative of the Hamilton function (Equation 17) for each variable state as follows:

$$\begin{aligned}
 \frac{d\lambda_1}{dt} &= -\frac{\partial H}{\partial S} = (\lambda_1 - \lambda_2) \left(\frac{(1-u_1)(\beta_1 I + \beta_2 C)}{N} + \frac{(1-u_1)(\beta_1 SI + \beta_2 SC)}{N^2} \right) \\
 &+ q_1(\lambda_1 - \lambda_5) + \lambda_1 \mu \\
 &+ \frac{\rho_1 \beta_1 QI}{N^2} (p\lambda_6 + (1-p)\lambda_7 - \lambda_5) \\
 &+ \frac{\rho_2 \beta_2 QC}{N^2} (q\lambda_6 + (1-q)\lambda_7 - \lambda_5), \\
 \frac{d\lambda_2}{dt} &= -\frac{\partial H}{\partial E} = (\lambda_2 - \lambda_1) \frac{(1-u_1)(CS\beta_2 + IS\beta_1)}{N^2} \\
 &+ \lambda_2 \alpha + \lambda_2 \mu - \lambda_3 \alpha \xi - \lambda_4 \alpha (1 - \xi) \\
 &+ \frac{\rho_1 \beta_1 QI}{N^2} (\lambda_6 p + (1-p)\lambda_7 - \lambda_5) + \frac{\rho_2 \beta_2 QC}{N^2} \\
 &(\lambda_6 q + (1-q)\lambda_7 - \lambda_5), \\
 \frac{d\lambda_3}{dt} &= -\frac{\partial H}{\partial I} = (\lambda_1 - \lambda_2) \left(\frac{(1-u_1)S\beta_1}{N} - \frac{(1-u_1)S\beta_1}{N} \right) \\
 &+ h_1(\lambda_3 - \theta\lambda_6 - (1-\theta)\lambda_7) \\
 &+ u_2(\lambda_3 - \lambda_6 - \lambda_7) + r_1(\lambda_3 - \lambda_8) - \lambda_3(-d_1 - \mu) \\
 &+ \frac{\rho_1 \beta_1 Q}{N} (\lambda_5 - \lambda_6 p - \lambda_7(1-p)) - 1, \\
 \frac{d\lambda_4}{dt} &= -\frac{\partial H}{\partial C} \\
 &= (\lambda_2 - \lambda_1) \left(-\frac{(1-u_1)S\beta_2}{N} + \frac{(1-u_1)(CS\beta_2 + IS\beta_1)}{N^2} \right) \\
 &+ h_2(\lambda_4 - \lambda_6 \delta - \lambda_7(1-\delta)) \\
 &+ r_2(\lambda_4 - \lambda_8) + u_2(\lambda_4 - \lambda_6 - \lambda_7) - \lambda_4(-d_2 - \mu) \\
 &+ \frac{\rho_1 \beta_1 QI}{N^2} (-\lambda_5 + \lambda_6 p + \lambda_7(1-p)) \\
 &+ \left(\frac{\rho_2 \beta_2 Q}{N} - \frac{\rho_2 \beta_2 QC}{N^2} \right) (\lambda_5 - \lambda_6 q - \lambda_7(1-q)) - 1, \\
 \frac{d\lambda_5}{dt} &= -\frac{\partial H}{\partial Q} = (\lambda_2 - \lambda_1) \left(\frac{(1-u_1)(CS\beta_2 + IS\beta_1)}{N^2} \right) \\
 &+ r_3(\lambda_5 - \lambda_8) \\
 &+ \left(\frac{\rho_1 \beta_1 I}{N} - \frac{\rho_1 \beta_1 QI}{N^2} \right) (\lambda_5 - p\lambda_6 - (1-p)\lambda_7) \\
 &+ \left(\frac{\rho_2 \beta_2 C}{N} - \frac{\rho_2 \beta_2 QC}{N^2} \right) (\lambda_5 - \lambda_6 q - \lambda_7(1-q)) + \lambda_5 \mu, \\
 \frac{d\lambda_6}{dt} &= -\frac{\partial H}{\partial H} = (\lambda_2 - \lambda_1) \left(\frac{(1-u_1)(CS\beta_2 + IS\beta_1)}{N^2} \right) \\
 &+ r_4(\lambda_6 - \lambda_8) + \frac{\rho_1 \beta_1 QI}{N^2} (-\lambda_5 + \lambda_6 p + \lambda_7(1-p)) \\
 &+ \frac{\rho_2 \beta_2 QC}{N^2} (-\lambda_5 + \lambda_6 q + \lambda_7(1-q)),
 \end{aligned}
 \tag{18}$$

$$\begin{aligned}
 \frac{d\lambda_7}{dt} &= -\frac{\partial H}{\partial J} = (\lambda_2 - \lambda_1) \left(\frac{(1-u_1)(CS\beta_2 + IS\beta_1)}{N^2} \right) \\
 &+ r_5(\lambda_7 - \lambda_8) + \frac{\rho_1 \beta_1 QI}{N^2} (-\lambda_5 + \lambda_6 p + \lambda_7(1-p)) \\
 &+ \frac{\rho_2 \beta_2 QC}{N^2} (-\lambda_5 + \lambda_6 q + \lambda_7(1-q)) + \lambda_7(d_4 + \mu), \\
 \frac{d\lambda_8}{dt} &= -\frac{\partial H}{\partial R} = (\lambda_2 - \lambda_1) \left(\frac{(1-u_1)(CS\beta_2 + IS\beta_1)}{N^2} \right) \\
 &+ \frac{\rho_1 \beta_1 QI}{N^2} (-\lambda_5 + \lambda_6 p + \lambda_7(1-p)) \\
 &+ \frac{\rho_2 \beta_2 QC}{N^2} (-\lambda_5 + \lambda_6 q + \lambda_7(1-q)) + \lambda_8 \mu.
 \end{aligned}$$

With transverse condition

$$\lambda_1(T) = \lambda_2(T) = \lambda_3(T) = \lambda_4(T) = \lambda_5(T) = \lambda_6(T) = \lambda_7(T) = \lambda_8(T) = 0.$$

The stationary condition for the optimal control problem (16) is obtained by deriving the Hamilton function (17) on the control variables u_1 and u_2 ($\frac{\partial \mathcal{H}}{\partial u_1} = 0, \frac{\partial \mathcal{H}}{\partial u_2} = 0$), successively obtained

$$\begin{aligned}
 u_1 &= \frac{(\beta_1 SI + \beta_2 SC)(\lambda_2 - \lambda_1)}{NA_1} \text{ and} \\
 u_2 &= \frac{I(\lambda_3 - \lambda_6 - \lambda_7) + C(\lambda_4 - \lambda_6 - \lambda_7)}{A_2}.
 \end{aligned}$$

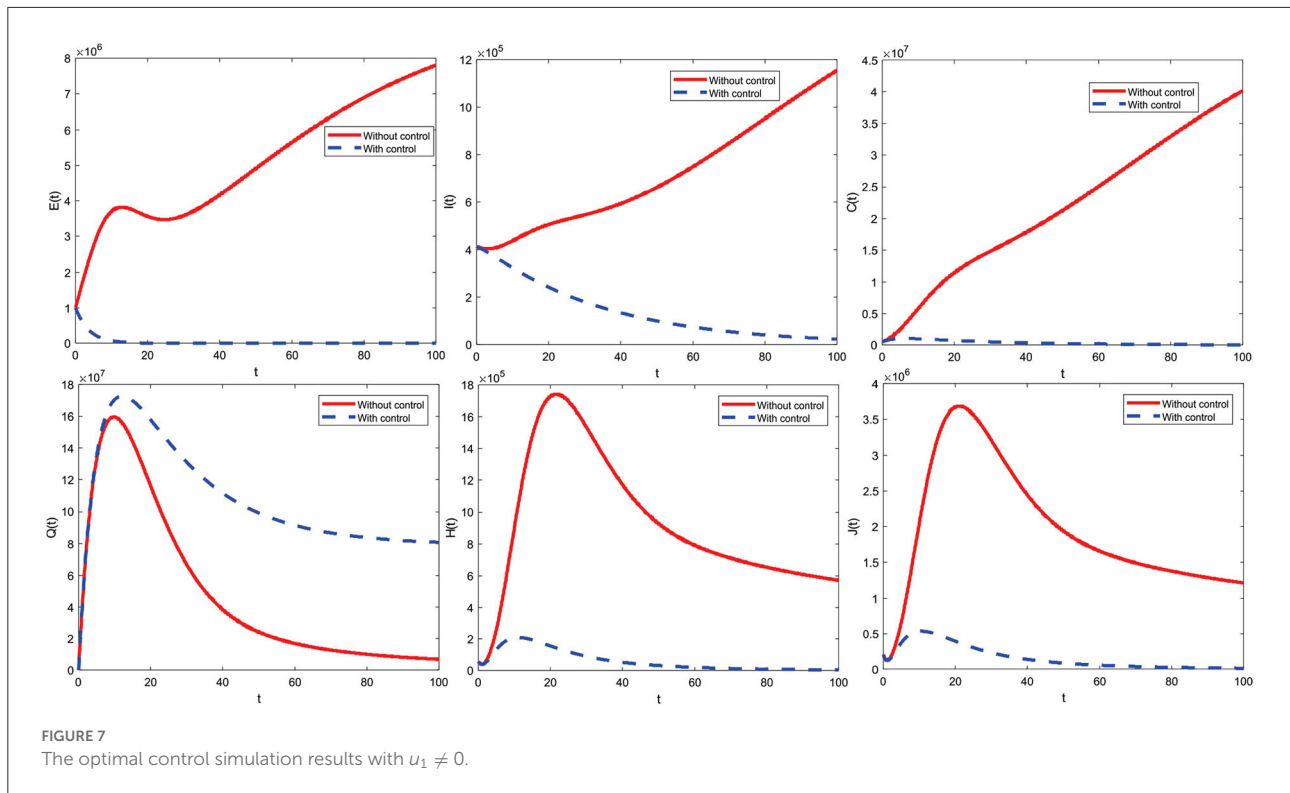
The control variables in the COVID-19 model with preventive measures through education and treatment efforts for infected individuals are defined as $0 \leq u_1 \leq 1$ and $0 \leq u_2 \leq 1$. So, the optimal control u_1^* and u_2^* can be expressed as

$$\begin{aligned}
 u_1^* &= \text{maks} \left\{ 0, \min \left(\frac{(\beta_1 S^* I^* + \beta_2 S^* C^*)(\lambda_2 - \lambda_1)}{NA_1}, 1 \right) \right\} \text{ and} \\
 u_2^* &= \text{maks} \left\{ 0, \min \left(\frac{I^*(\lambda_3 - \lambda_6 - \lambda_7) + C^*(\lambda_4 - \lambda_6 - \lambda_7)}{A_2}, 1 \right) \right\}.
 \end{aligned}$$

The optimal system is obtained by substituting the optimal control variables u_1^* and u_2^* into the system of state (Equation 15) and costate (Equation 18) equations.

6. Simulation of the model with control

The method used in solving this optimal control problem is the forward-backward sweep method. In this numerical simulation, the parameter values used are presented in Table 1 according to the state of the COVID-19 case in Indonesia. Next, the initial values given are as follows $S_0 = 270,911,990, E_0 = 1,000,000, I_0 = 412,784, C_0 = 500,000, Q_0 = 100,000, H_0 = 56,899, J_0 = 200,000,$ and $R_0 = 341,942,$ with simulation intervals $t \in [0, 100]$. The results of the optimal numerical control simulation are presented as follows:



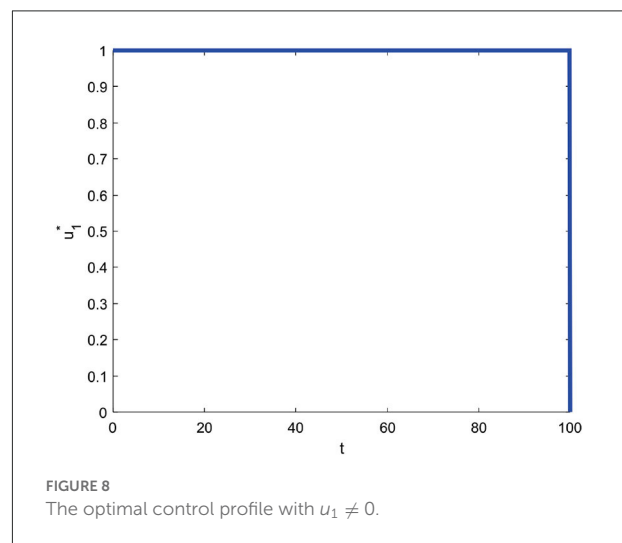
6.1. Using the control strategy $u_1 \neq 0$ and $u_2 = 0$

Figure 7 shows the control strategy $u_1 \neq 0$ and $u_2 = 0$. This is the result of education that makes all individuals always be careful, such as interacting outside the home. Implementing this strategy on subpopulations exposed, infected with comorbidity, infected without comorbidity, and isolation is significantly reduced. Implementing the control strategy $u_1 \neq 0$ and $u_2 = 0$ can also increase the subpopulation of quarantine. Furthermore, the control strategy profiles $u_1 \neq 0$ and $u_2 = 0$ to reduce the number of COVID-19 cases during $t = 100$ are presented in Figure 8.

The control strategy $u_1 \neq 0$ and $u_2 = 0$ is given by one (maximum) from the beginning of the period to $t = 99.9$ and decreases significantly to zero at the end of the period. Control is terminated at the period's end, meaning no more control is given.

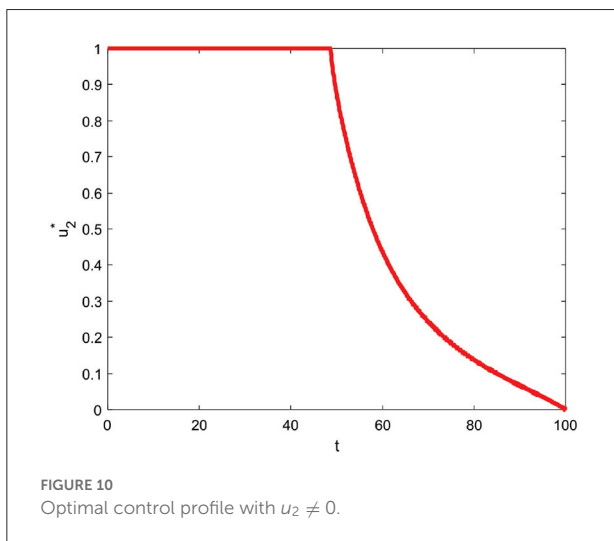
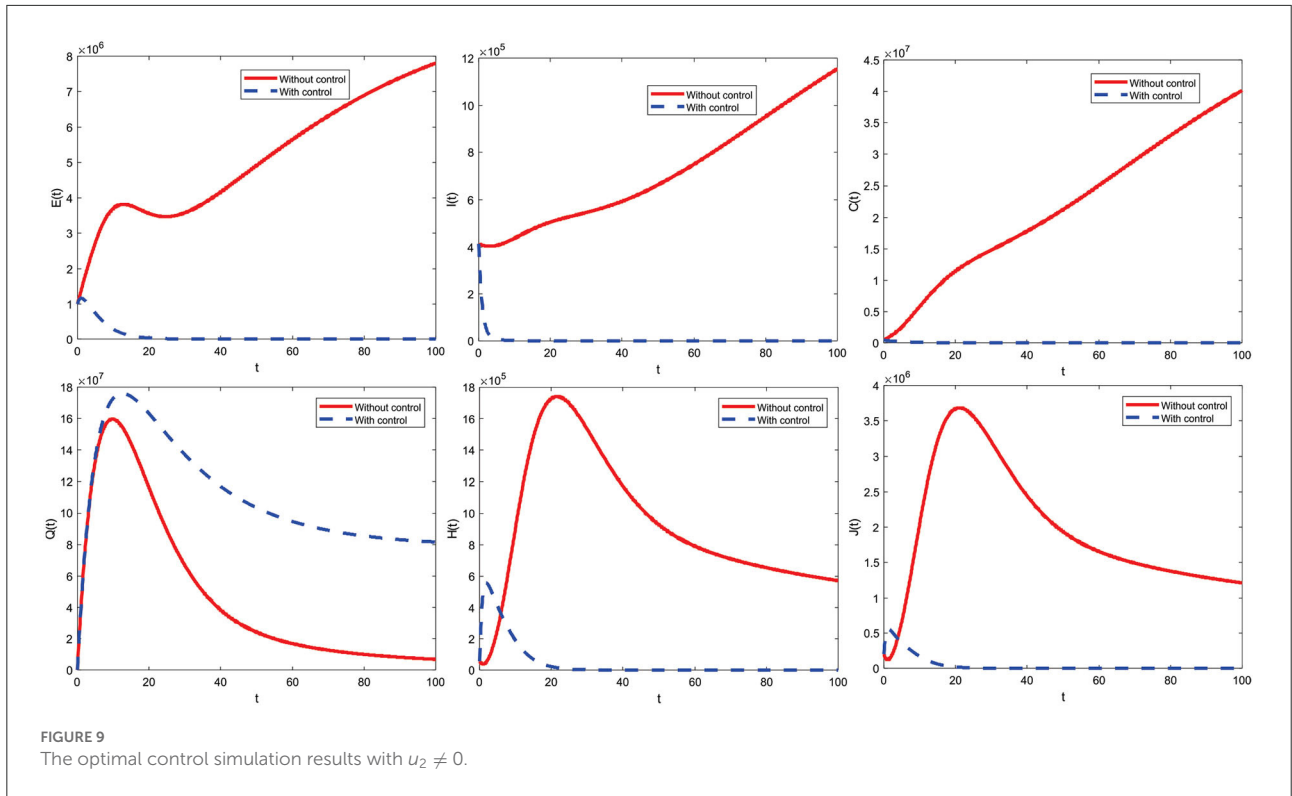
6.2. Using the control strategy $u_1 = 0$ and $u_2 \neq 0$

Figure 9 shows the control strategy $u_1 = 0$ and $u_2 \neq 0$. This strategy can reduce the subpopulation infected with comorbid and without comorbid because there is an increase in the care of infected individuals. Implementing this strategy



on subpopulations exposed, infected with comorbidity, infected without comorbidity, and isolation is significantly reduced. Implementing the control strategies $u_1 = 0$ and $u_2 \neq 0$ can also increase the subpopulation of quarantine. Furthermore, the profiles of $u_1 = 0$ and $u_2 \neq 0$ control strategies to reduce the number of COVID-19 cases for $t = 100$ are presented in Figure 10.

The control strategy $u_1 = 0$ and $u_2 \neq 0$ is given by one (maximum) from the beginning to $t = 48.6$ and decreases slowly



until $t = 100$ reaches zero which means control is stopped at the end of the period.

6.3. Using the control strategy $u_1 \neq 0$ and $u_2 \neq 0$

Figure 11 indicates a combined control strategy. This results from education that makes all individuals always be careful (such

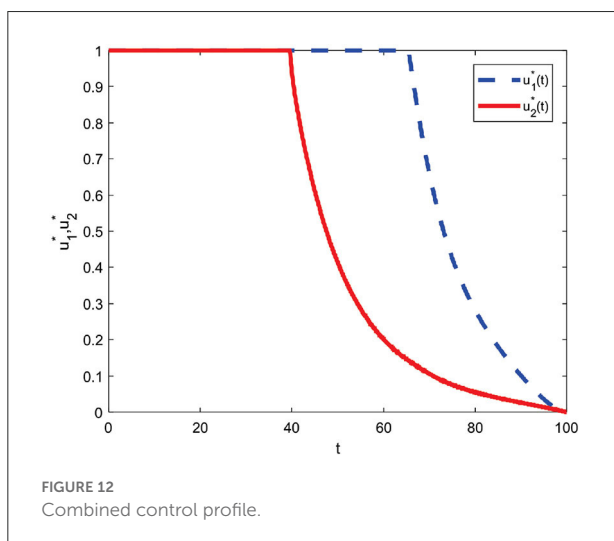
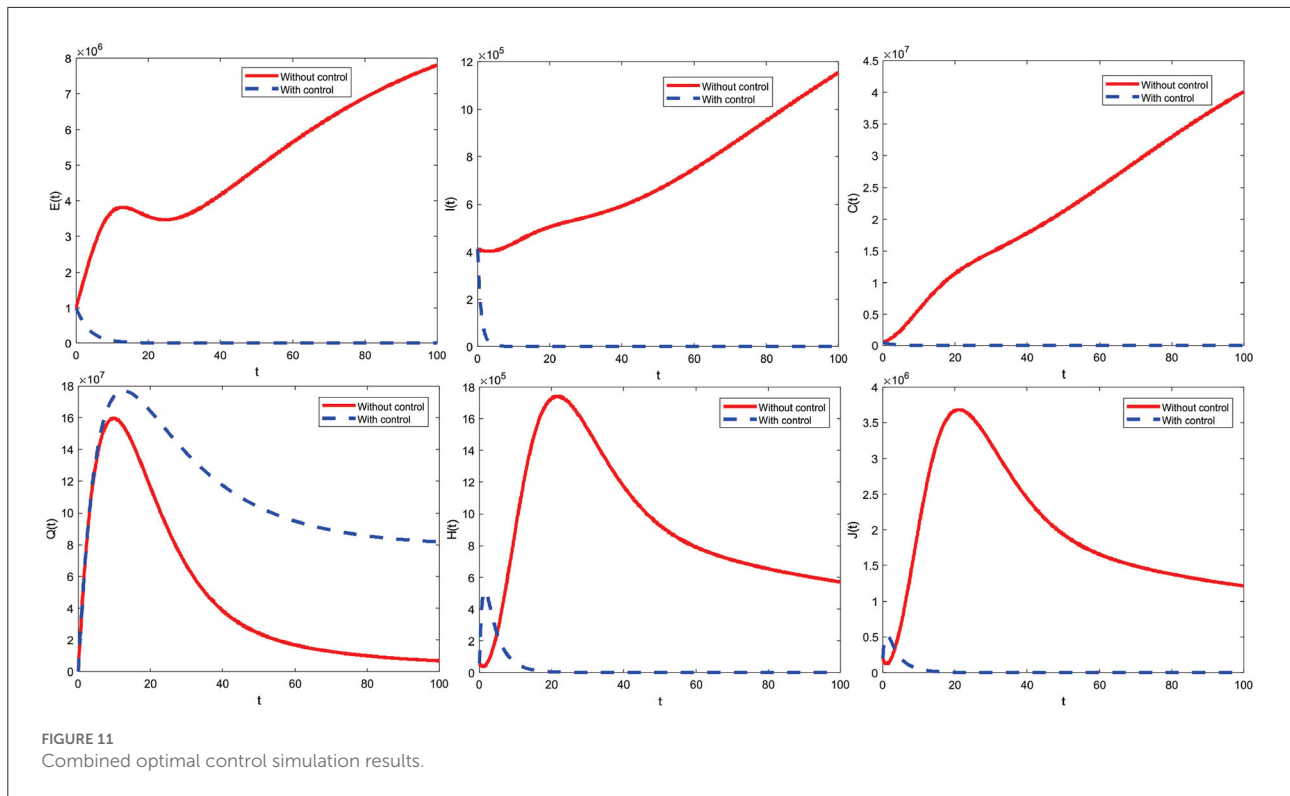
as interacting outside the home) and increased care for infected individuals. Combined control strategies can control or reduce deployment significantly. Furthermore, the combined control strategy profile to reduce the number of COVID-19 cases during $t = 100$ is presented in Figure 12.

The combined control strategy consists of two concurrent administrations of control. The control u_1 is given by one (maximum) up to $t = 65.4$ and decreases significantly until the end of the period reaches zero. Then, control u_2 is assigned one (maximum) until $t = 39.5$ and then decreases until $t = 100$ slowly reaches zero. Both controls are terminated at the end of the period, which means they are no longer given control of u_1 and u_2 .

6.4. Comparison of total infections using all strategic control scenarios

The varying initial values of the exposed subpopulations are given. Total infected subpopulations for different initial conditions from exposed subpopulations are $E(0) = 200000, E(0) = 1000000, E(0) = 10000000$, and $E(0) = 100000000$ successively from left to right using the three control strategies shown in Figure 13.

From Figure 13, it can be seen that the number of infected subpopulations was reduced by applying the third strategy compared to other strategies. Based on strategies 1–3, it can be



concluded that strategy 3 is the best strategy to minimize the number of people infected with COVID-19 in the community.

7. Cost evaluation

The cost evaluation aims to determine the most minimal cost-effectiveness strategy of COVID-19 spread control

measures. Cost evaluation in this study uses average cost-effectiveness ratio (ACER) and incremental cost-effectiveness ratio (ICER). According to the approach to cost-effectiveness analysis, ACER is defined mathematically as follows:

$$ACER = \frac{\text{Objective function } (J)}{\text{Total number of infections averted}}$$

The strategy with the smallest ACER value is the most cost-effective and is obtained in Table 4 as follows:

The incremental cost-effectiveness ratio, which compares two intervention options vying for the same scarce resources, typically tracks costs and health benefits changes. ICER is defined as follows when considering strategies *p* and *q* as two competing control intervention techniques:

$$ICER = \frac{\text{Change in total costs in strategies p and q}}{\text{Change in control benefits in strategies p and q}}$$

Next, ICER was calculated to determine the most cost-effective strategy out of all the control strategies. First, the competition for strategies 1 and 2 is calculated as follows:

$$ICER(1) = \frac{49,247,000,000 - 0}{53,846,000,000 - 0} = 0.9146,$$

$$ICER(2) = \frac{2,991,000,000 - 49,247,000,000}{53,893,000,000 - 46,256,000,000} = -984.1702,$$

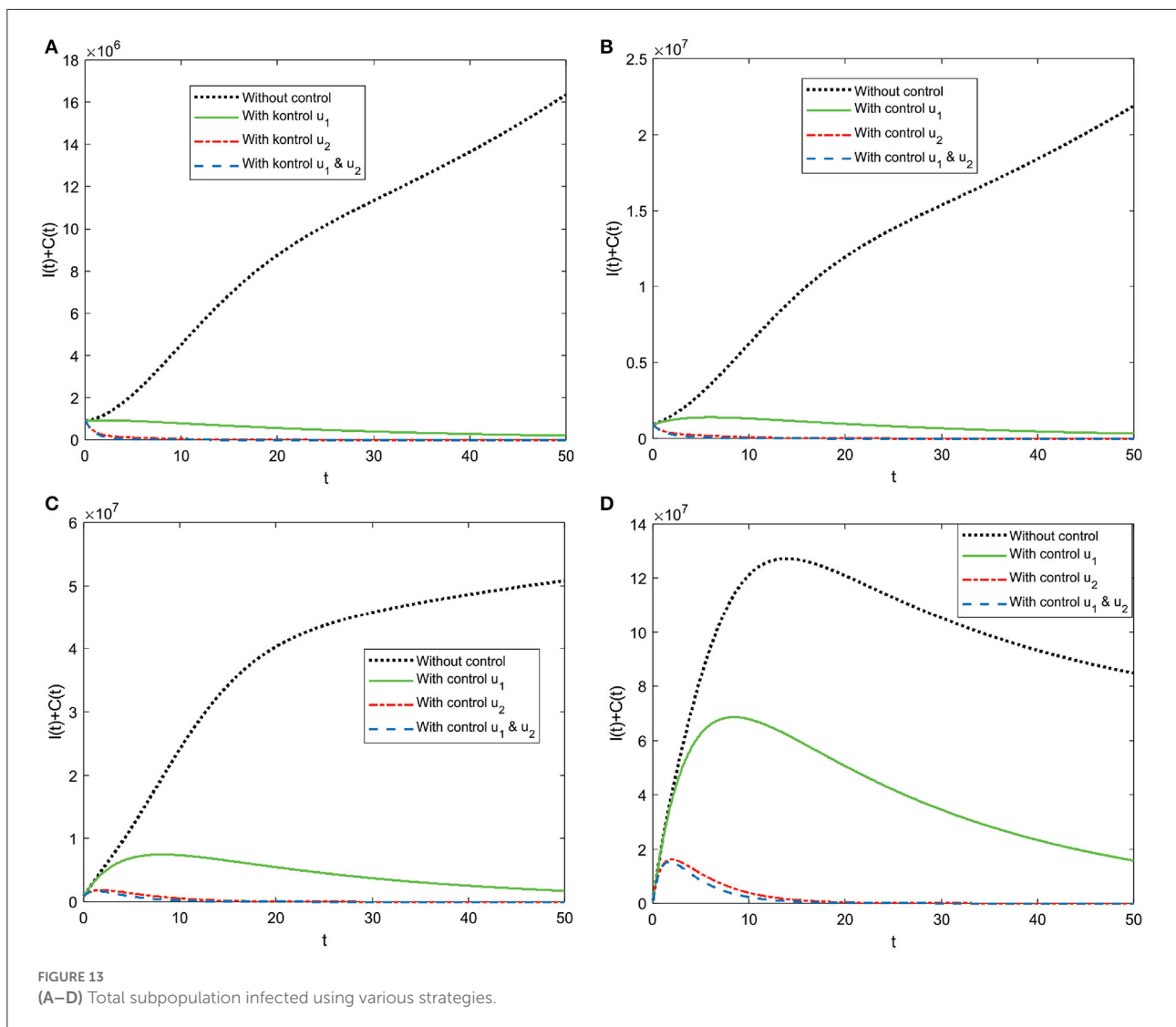


FIGURE 13 (A–D) Total subpopulation infected using various strategies.

The ICER results in strategy 1 were greater than in strategy 2, so educational controls alone were more expensive and ineffective than medical care enhancement controls. Therefore, strategy 1 is removed from the possible control strategies. Next, the ICER for strategies 2 and 3 is recalculated as follows:

$$ICER(2) = \frac{2,991,000,000 - 0}{53,893,000,000 - 0} = 0.5130,$$

$$ICER(3) = \frac{1,794,700,000 - 2,991,000,000}{53,894,000,000 - 53,893,000,000} = -\frac{1,196,300,000}{1,000,000} = -1,196.3.$$

Strategy 2 has a higher ICER value than strategy 3. So, strategy 3 (combined control) is the best control strategy of all options because of its cost-effectiveness and prevention of the spread of infectious diseases.

TABLE 4 Total infections prevented, total costs, and ACER for strategies 1, 2, and 3.

Strategy	Infections prevented	Total cost	ACER
No strategy	0	0	0
Strategy 1	53,846,000,000	49,247,000	0.9146
Strategy 2	53,893,000,000	2,991,000	0.0555
Strategy 3	53,894,000,000	1,794,700	0.0333

8. Conclusion

In this study, we have proposed a mathematical model of COVID-19 with comorbidities and added control of community education and improvement of medical care. The proposed

model has been calibrated using cumulative confirmed infection cases in Indonesia. The basic reproduction number has been calculated by the next-generation matrix method. The model has an asymptotically stable disease-free equilibrium, provided that the basic reproduction number is <1 . Furthermore, the model has an asymptotically stable endemic equilibrium, provided that the basic reproduction number is more than one. Individuals with comorbidity have a greater risk of infection, so there is a need for more supervision and preventive measures such as wearing masks, maintaining distance, and proper sanitation. Public education can be through social media, TV, radio, print media, and others to control the COVID-19 pandemic in Indonesia. Based on the model analysis, it is found that the COVID-19 pandemic can be controlled and eradicated if the value of $R_0 < 1$ by providing public education control and improving medical care. The sensitivity analysis results show that the most influential parameters are quarantine and contact with infected individuals, so educating the public to reduce disease transmission is important. After public education was given, the community became aware of the COVID-19 outbreak and began to reduce contact with other people. Likewise, the Indonesian government imposed large-scale social restrictions (PSBB) and enforced restrictions on community activities (PPKM) with four levels aiming to reduce infection and reduce social contact, educational institutions conducted online classes, webinars, etc. In addition to public education, increased medical care also need to be given to individuals who are already infected so that they recover quickly and that the epidemic is resolved soon. Furthermore, from the numerical results and cost-effectiveness analysis on the optimal control problem, it is found that applying a combination of controls can give the best results compared to a single control. This study can be extended in various ways, including considering the stochastic, time delay, and fractional derivative versions of this model. In addition, providing control variations (such as

the presence of vaccination) combines the dynamics of two COVID-19 strains with another comorbidity and considers the COVID-19 vaccination model.

Data availability statement

The raw data supporting the conclusions of this article will be made available by the authors, without undue reservation.

Author contributions

MAR and F: conceptualization. MAR: methodology, software, writing—original draft preparation, and visualization. MAR, F, CA, and CWC: validation, investigation, and data curation. F, CA, and CWC: formal analysis. MAR, F, and CA: writing—review and editing. F and CA: supervision. All authors have read and agreed to the published version of the manuscript.

Conflict of interest

The authors declare that the research was conducted in the absence of any commercial or financial relationships that could be construed as a potential conflict of interest.

Publisher's note

All claims expressed in this article are solely those of the authors and do not necessarily represent those of their affiliated organizations, or those of the publisher, the editors and the reviewers. Any product that may be evaluated in this article, or claim that may be made by its manufacturer, is not guaranteed or endorsed by the publisher.

References

1. WHO. *Novel Coronavirus*. (2020). Available online at: <https://www.who.int/indonesia/news/novel-coronavirus>
2. Wu Z, McGoogan JM. Characteristics of and important lessons from the coronavirus disease 2019 (COVID-19) outbreak in China: summary of a report of 72 314 cases from the Chinese center for disease control and prevention. *JAMA*. (2020) 323:1239–42. doi: 10.1001/jama.2020.2648
3. Kemkes. *Pertanyaan dan Jawaban Terkait COVID-19 Kementerian Kesehatan*. (2020). Available online at: <https://www.kemkes.go.id/article/view/20030400008/FAQ-Coronavirus.html>
4. WHO. *Novel Coronavirus (COVID-19)*. (2021). Available online at: <https://www.moh.gov.sa/en/HealthAwareness/EducationalContent/Corona/Pages/corona.aspx>
5. WHO. *Novel Coronavirus (2019-nCoV): Situation Report 1*. (2020). Available online at: <https://apps.who.int/iris/handle/10665/330760>
6. Wu YC, Chen CS, Chan YJ. The outbreak of COVID-19: an overview. *J Chin Med Assoc*. (2020) 83:217–20. doi: 10.1097/JCMA.0000000000000270
7. Guan W, Liang W, Zhao Y, Liang H, Chen Z, Li Y, et al. Comorbidity and its impact on 1590 patients with COVID-19 in China: a nationwide analysis. *Eur Respir J*. (2020) 55:2000547. doi: 10.1183/13993003.00547-2020
8. Yang J, Zheng Y, Gou X, Pu K, Chen Z, Guo Q. International journal of infectious diseases prevalence of comorbidities and its effects in patients infected with SARS-CoV-2: a systematic review and meta-analysis. *Int J Infect Dis*. (2020) 94:91–5. doi: 10.1016/j.ijid.2020.03.017
9. Satgas. *Peta Sebaran COVID-19*. (2021). Available online at: <https://covid19.go.id/peta-sebaran>
10. Adisasmito W, Suwandono A, Trihono, Gani A, Aisyah DN, Solikha DA, et al. Studi komparasi pembelajaran penanganan COVID-19 Indonesia-Korea Selatan. In: *Direktorat Kesehatan dan Gizi Masyarakat Kementerian PPN/BAPPENAS*. (2021). Available online at: <https://infeksiemerging.kemkes.go.id/document/download/3ax61Bxrn5>
11. Worldometers. *Report Coronavirus Cases* (2021). Available online at: <https://www.worldometers.info/coronavirus/>

12. Lemon SM, Hamburg MA, Frederick B, Choffnes ER, Mack A. *Ethical and Legal Considerations in Mitigating Pandemic Disease: Workshop Summary*. Washington, DC: National Academic Press (2007).
13. WHO. *COVID-19 Strategy Update*. (2020). Available online at: <https://www.who.int/publications/m/item/covid-19-strategy-update>
14. WHO. *Pertimbangan-Pertimbangan Untuk Karantina Individu Dalam Konteks Penanggulangan Penyakit Coronavirus (COVID-19)*. (2020). Available online at: https://www.who.int/docs/default-source/searo/indonesia/covid19/who-2019-covid19-ihq-quarantine-2020-indonesian.pdf?sfvrsn=31d7cbd8_2
15. Tang B, Wang X, Li Q, Bragazzi NL, Tang S, Xiao Y, et al. Estimation of the transmission risk of the 2019-nCoV and its implication for public health interventions. *J Clin Med*. (2020) 9:462. doi: 10.3390/jcm9020462
16. Müller J, Kuttler C. *Methods and Models in Mathematical Biology*. Berlin; Heidelberg: Springer-Verlag (2015).
17. Murray JD. *Mathematical Biology I: An Introduction*. Berlin; Heidelberg: Springer-Verlag (2002).
18. Feng Z. Final and peak epidemic sizes for SEIR models with quarantine and isolation. *Math Biosci Eng*. (2007). 4:675–86. doi: 10.3934/mbe.2007.4.675
19. Tahir M, Shah SIA, Zaman G, Khan T. Stability behaviour of mathematical model MERS corona virus spread in population. *Filomat*. (2019) 33:3947–60. doi: 10.2298/FIL1912947T
20. Usaini S, Hassan AS, Garba SM, Lubuma JMS. Modeling the transmission dynamics of the middle east respiratory syndrome coronavirus (MERS-CoV) with latent immigrants. *J Interdisc Math*. (2019) 22:903–30. doi: 10.1080/09720502.2019.1692429
21. Soewono E. On the analysis of COVID-19 transmission in wuhan, diamond princess and jakarta-cluster. *Commun Biomath Sci*. (2020) 3:9–18. doi: 10.5614/cbms.2020.3.1.2
22. Das P, Upadhyay RK, Misra AK, Rihan FA, Das P, Ghosh D. Mathematical model of COVID-19 with comorbidity and controlling using non-pharmaceutical interventions and vaccination. *Nonlinear Dyn*. (2021) 106:1213–27. doi: 10.1007/s11071-021-06517-w
23. Omame A, Sene N, Nometa I, Nwakanma CI, Nwafor EU, Iheonu NO, et al. Analysis of COVID-19 and comorbidity co-infection model with optimal control. *Optimal Control Appl Methods*. (2021) 42:1568–90. doi: 10.1002/oca.2748
24. Jia J, Ding J, Liu S, Liao G, Li J, Duan B, et al. Modeling the control of COVID-19: impact of policy interventions and meteorological factors. *Electron J Diff Equ*. (2020) 2020:23.
25. Prathumwan D, Trachoo K, Chaiya I. Mathematical modeling for prediction dynamics of the coronavirus disease 2019 (COVID-19) pandemic, quarantine control measures. *Symmetry*. (2020) 12:1404. doi: 10.3390/sym12091404
26. Deressa CT, Duressa GF. Modeling and optimal control analysis of transmission dynamics of COVID-19: The case of Ethiopia. *Alexandria Eng J*. (2020) 60:719–32. doi: 10.1016/j.aej.2020.10.004
27. Olaniyi S, Obabiyi OS, Okosun KO, Oladipo AT, Adewale SO. Mathematical modelling and optimal cost-effective control of COVID-19 transmission dynamics. *Eur Phys J Plus*. (2020) 135:938. doi: 10.1140/epjp/s13360-020-00954-z
28. Aldila D, Khoshnaw SHA, Safitri E, Rais YA, Bakry ARQ, Samiadji BM, et al. A mathematical study on the spread of COVID-19 considering social distancing and rapid assessment: the case of Jakarta, Indonesia. *Chaos Solit Fractals*. (2020) 139:110042. doi: 10.1016/j.chaos.2020.110042
29. Aldila D, Ndii MZ, Samiadji BM. Optimal control on COVID-19 eradication program in Indonesia under the effect of community awareness. *Math Biosci Eng*. (2020) 17:6355–89. doi: 10.3934/mbe.2020335
30. Ali M, Shah STH, Imran M, Khan A. The role of asymptomatic class, quarantine and isolation in the transmission of COVID-19. *J Biol Dyn*. (2020) 14:389–408. doi: 10.1080/17513758.2020.1773000
31. Rois MA, Tafrikan M, Norasia Y, Anggriani I, Ghani M. SEIHR model on spread of COVID-19 and its simulation. *Telematika*. (2022) 15.
32. Annas S, Pratama MI, Rifandi M, Sanusi W, Side S. Stability analysis and numerical simulation of SEIR model for pandemic COVID-19 spread in Indonesia. *Chaos Solit Fractals*. (2020) 139:110072. doi: 10.1016/j.chaos.2020.110072
33. Baba IA, Nasidi BA, Baleanu D. Optimal control model for the transmission of novel COVID-19. *Comput Mater Continua*. (2021) 66:3089–106. doi: 10.32604/cmc.2021.012301
34. Li XP, Darassi MH, Khan MA, Chukwu CW, Alshahrani MY, Shahrani MA, et al. Assessing the potential impact of COVID-19 Omicron variant: insight through a fractional piecewise model. *Results Phys*. (2022) 38:105652. doi: 10.1016/j.rinp.2022.105652
35. Bajjiya VP, Bugalia S, Tripathi JP. Mathematical modeling of COVID-19: impact of non-pharmaceutical interventions in india mathematical modeling of COVID-19: impact of non-pharmaceutical interventions in India. *Chaos*. (2020) 30:113143. doi: 10.1063/5.0021353
36. Das P, Nadim SS, Das S, Das P. Dynamics of COVID-19 transmission with comorbidity: a data driven modelling based approach. *Nonlinear Dyn*. (2021) 106:1197–211. doi: 10.1007/s11071-021-06324-3
37. Diagne ML, Rwezaura H, Tchoumi SY, Tchuenche JM. Mathematical model of COVID-19 with vaccination and treatment. *Comput Math Methods Med*. (2021) 2021:1250129. doi: 10.1155/2021/1250129
38. Ghostine R, Gharamti M, Hassrouny S, Hoteit I. An extended SEIR model with vaccination for forecasting the COVID-19 pandemic in Saudi Arabia using an ensemble Kalman filter. *Mathematics*. (2021) 9:636. doi: 10.3390/math9060636
39. Kouidere A, Khajji B, Bhil AE, Balatif O, Rachik MA. Mathematical modeling with optimal control strategy of transmission of COVID-19 pandemic virus. *Commun Math Biol Neurosci*. (2020) 2020:24. doi: 10.28919/cmbn/4599
40. Madubueze CE, Onwubuya IO, Dachollom S. Controlling the spread of COVID-19: optimal control analysis. *Comput Math Methods Med*. (2020) 2020:6862516. doi: 10.1101/2020.06.08.20125393
41. Naveed M, Baleanu D, Rafiq M, Raza A, Soori A, Hasan, et al. Dynamical behavior and sensitivity analysis of a delayed coronavirus epidemic model. *Comput Mater Continua*. (2020) 65:225–41. doi: 10.32604/cmc.2020.011534
42. Riyapan P, Shuaib SE, Intarasit A. A mathematical model of COVID-19 pandemic: a case study of Bangkok, Thailand. *Comput Math Methods Med*. (2021) 2021:6664483. doi: 10.1155/2021/6664483
43. Yang C, Wang J. A mathematical model for the novel coronavirus epidemic in Wuhan, China. *Math Biosci Eng*. (2020) 17:2708–24. doi: 10.3934/mbe.2020148
44. Youssef HM, Alghamdi NA, Ezzat MA, El-bary AA, Shawky AM. Study on the SEIQR model and applying the epidemiological rates of COVID-19 epidemic spread in Saudi Arabia. *Infect Dis Model*. (2021) 6:678–92. doi: 10.1016/j.idm.2021.04.005
45. Youssef HM, Alghamdi NA, Ezzat MA, El-Bary AA, Shawky AM. A new dynamical modeling SEIR with global analysis applied to the real data of spreading COVID-19 in Saudi Arabia. *Math Biosci Eng*. (2020) 17:7018–44. doi: 10.3934/mbe.2020362
46. Rois MA, Trisilowati T, Habibah U. Dynamic analysis of COVID-19 model with quarantine and isolation. *JTAM*. (2021) 5:418–33.
47. Rois MA, Trisilowati, Habibah U. Optimal control of mathematical model for COVID-19 with quarantine and isolation. *Int J Eng Trends Technol*. (2021) 69:154–60. doi: 10.14445/22315381/IJETT-V69I6P223
48. Musa SS, Qureshi S, Zhao S, Yusuf A, Mustapha UT, He D. Mathematical modeling of COVID-19 epidemic with effect of awareness programs. *Infect Dis Model*. (2021) 6:448–60. doi: 10.1016/j.idm.2021.01.012
49. Chukwu CW, Fatmawati. Modelling fractional-order dynamics of COVID-19 with environmental transmission and vaccination: a case study of Indonesia. *AIMS Math*. (2022) 7:4416–38. doi: 10.3934/math.2022246
50. Zeb A, Alzahrani E, Erturk VS, Zaman G. Mathematical Model for coronavirus disease 2019 (COVID-19) containing isolation class. *BioMed Res Int*. (2020) 2020:3452402. doi: 10.1155/2020/3452402
51. Bonyah E, Juga M, Fatmawati. Fractional dynamics of coronavirus with comorbidity via Caputo-Fabrizio derivative. *Commun Math Biol Neurosci*. (2022) 2022:12. doi: 10.28919/cmbn/6964
52. Fatmawati, Yuliani E, Alfiniyah C, Juga ML, Chukwu CW. On the modeling of COVID-19 transmission dynamics with two strains: insight through caputo fractional derivative. *Fractal Fract*. (2022) 6:346. doi: 10.3390/fractalfract6070346
53. Majumder M, Tiwari PK, Pal S. Impact of saturated treatments on HIV-TB dual epidemic as a consequence of COVID-19: optimal control with awareness and treatment. *Nonlinear Dyn*. (2022) 109:143–76. doi: 10.1007/s11071-022-03795-6
54. Rai RK, Khajanchi S, Tiwari PK, Venturino E, Misra AK. Impact of social media advertisements on the transmission dynamics of COVID-19 pandemic in India. *J Appl Math Comput*. (2022) 68:19–44. doi: 10.1007/s12190-021-01507-y
55. Brauer F, Castillo-Chavez C. *Mathematical Models in Population Biology and Epidemiology*. New York, NY: Springer-Verlag New York (2012).
56. Driessche PVD, Watmough J. Reproduction numbers and sub-threshold endemic equilibria for compartmental models of disease transmission. *Math Biosci*. (2002) 180:29–48. doi: 10.1016/S0025-5564(02)00108-6
57. Alligood KT, Sauer TD, Yorke JA. CHAOS: an Introduction to dynamical systems. In: *Introduction To Computational Modeling Using C and Open-Source Tools*. New York, NY; Berlin; Heidelberg: Springer-Verlag (2000).
58. Chitnis N, Hyman JM, Cushing JM. Determining important parameters in the spread of malaria through the sensitivity analysis of a mathematical model. *Bull Math Biol*. (2008) 70:1272. doi: 10.1007/s11538-008-9299-0
59. Rois MA, Trisilowati T, Habibah U. Local sensitivity analysis of COVID-19 epidemic with quarantine and isolation using normalized index. *Telematika*. (2021) 14:13–24. doi: 10.35671/telematika.v14i1.1191